THE ASTROPHYSICAL JOURNAL, 427:1013–1034, 1994 June 1

THE EFFECTIVENESS OF OSCILLATION FREQUENCIES IN CONSTRAINING STELLAR MODEL PARAMETERS

TIMOTHY M. BROWN
High Altitude Observatory/National Center for Atmospheric Research,[1] P.O. Box 3000, Boulder, CO 80307

J. CHRISTENSEN-DALSGAARD
High Altitude Observatory/National Center for Atmospheric Research, and Institut for Fysik og Astronomi, Aarhus Universitet, DK-8000 Aarhus C, Denmark[2]

BARBARA WEIBEL-MIHALAS
National Center for Supercomputing Applications, 605 E. Springfield Avenue, Urbana, IL 61820

AND

RONALD L. GILLILAND
Space Telescope Science Institute, 3700 San Martin Drive, Baltimore, MD 21218
Received 1993 September 13; accepted 1993 November 22

ABSTRACT

Recent observational advances suggest that it may soon be possible to measure the frequencies of *p*-mode oscillations on distant Sun-like stars. We investigate the potential utility of such oscillation frequencies in determining the fundamental stellar structure parameters of these stars, in the case in which frequencies may be measured for both members of a visual binary system. To utilize all of the observations presumed to be available in an optimal way, we develop a formalism based on singular value decomposition (SVD) to relate errors in observed quantities to those in model parameters. As a particularly interesting example, we consider the α Cen system as it would be seen from distances between 1.3 pc (its true distance) and 100 pc. We find that for the nearest case, adding oscillation frequency separations with plausible errors to the available astrometric, photometric, and spectroscopic data allows one to reduce the formal errors in estimates of the helium abundance, heavy-element abundance, and mixing length by roughly a factor of 2. Estimates of the stellar masses and the system's age and distance are not markedly improved, mostly because of the very high quality astrometric data that can be obtained on such a nearby object. If the system were located at a significantly larger distance, the addition of oscillation information would allow drastic reductions in the formal error applicable to all of the stellar parameters except the helium abundance. These results suggest that accurately measured oscillation frequencies for visual binaries might allow tests of stellar structure theory at a level of precision that has hitherto been obtainable only for a few eclipsing binaries. Reducing the observational errors in photometry or astrometry by a factor of 3 does not provide the same level of improvement, especially for relatively distant systems. We show that the extra information contained in the oscillation frequencies for a reasonable set of modes would easily allow one to distinguish between models using opacity laws obtained from the Los Alamos Opacity Library and from the more recent Livermore OPAL tables. Different formulations of the equation of state (without and with Coulomb effects) lead to models that are marginally distinguishable, while models with and without helium settling from the convection zone are not distinguishable, given observations with errors as large as we assume.

Subject headings: stars: abundances — stars: fundamental parameters — stars: interiors — stars: oscillations

1. INTRODUCTION

In the last decade, observations of *p*-mode pulsations in the Sun have been successfully interpreted to yield a wealth of information about the nearest star. It is natural to suppose that information about similar pulsations on other Sun-like stars would significantly improve our knowledge about those objects as well, even though the lack of spatial resolution severely limits the number of stellar oscillation modes that might be observed. Such improvements would of course be highly desirable. For example, knowledge of the most basic parameters of stellar structure (mass, age, and composition) for a suitable sample of stars has a direct bearing on our understanding of the age and chemical evolution of the Galaxy. Even more directly, accurate oscillation data might provide a confrontation with the theory of stellar structure; by comparing observed frequencies (and other stellar observables) with those predicted by theory, one may hope to assess the importance of phenomena that are not included in traditional treatments of stellar evolution.

Technical advances suggest that stellar *p*-modes might soon be observable on a number of nearby solar-like stars, albeit with considerable difficulty (e.g., Gelly, Grec, & Fossat 1986; Brown et al. 1991; Innes et al. 1991; Pottasch, Butcher, & van Hoesel 1992; Gilliland et al. 1993). It therefore is of interest to know exactly what information can and cannot be extracted from the oscillation data that might plausibly be obtained, or from such data in combination with observations of other kinds. Some efforts in this direction have been made for the case of isolated stars (Ulrich 1986; Christensen-Dalsgaard 1984, 1988; Gough 1987, 1990a). Rather than deal with the frequencies of individual modes, these authors formulated their

[1] The National Center for Atmospheric Research is sponsored by the National Science Foundation.
[2] Permanent address.

analysis in terms of two frequency differences, or *separations*. The first of these is termed $\Delta\nu_0$ (or the *large separation*) and is defined as the mean frequency difference between modes that have the same angular degree l, but that differ by one in their radial order n. According to asymptotic theory (Vandakurov 1967; Tassoul 1980), this separation is equal to the reciprocal of the sound travel time across the star. This quantity is also closely related to the star's mean density $\bar{\rho}$. For stars with similar central condensation, one may write with good accuracy

$$\Delta\nu_0 \equiv \nu(n+1, l) - \nu(n, l) = 135\left(\frac{\bar{\rho}_\odot}{\bar{\rho}}\right)^{1/2} \mu\text{Hz}\,, \qquad (1)$$

where $\bar{\rho}_\odot$ is the solar mean density. The second frequency separation considered is the *small separation* $\delta\nu_0$, which is defined to be the frequency difference

$$\delta\nu_0 \equiv \nu(n+1, l=0) - \nu(n, l=2)\,. \qquad (2)$$

According to lowest order asymptotic theory, this frequency difference should be exactly zero. When higher order asymptotic terms are taken into account, the apparent frequency degeneracy is lifted, because of differences in the way modes with $l = 0$ and $l = 2$ propagate in the very deepest parts of the star. The small separation $\delta\nu_0$ therefore measures conditions in and near the stellar core, and in particular is sensitive to age-related changes in the core's chemical composition.

Ulrich (1986) and Christensen-Dalsgaard (1984, 1988) concluded that measurements of both $\Delta\nu_0$ and $\delta\nu_0$ could be combined to give estimates of both the mass and age of an isolated star, and that if other information about the star (for example, its surface gravity) were available, then something might be learned about the convective mixing length or the composition. Gough (1987, 1990a) challenged these conclusions, pointing out that the mass and age estimates depend sensitively on the stellar composition, especially the relatively poorly determined heavy-element abundance Z. He therefore argued that stellar mass and age could not be determined to useful precision from the two frequency separations alone; other information would be required to make accurate parameter determinations.

The fundamental difficulty underlying parameter estimation for isolated stars is that the number of precisely observable quantities (even including frequency separations) is not large compared to the number of model parameters one must consider. One thus expects that whole families of stellar models may fit the observations equally well, so that at least some of the stellar parameters must be very poorly determined. To avoid this unhappy situation, one must evidently consider contexts in which there are many more observables, but only a few more unknown parameters.

One such case is that of a visual binary system. For a detached visual binary with two main-sequence components, one may reasonably assume that both stars have the same age and the same initial composition, and that mass transfer between the stars has never been important. Relative to a single star, the only new parameters to consider are the mass of the second component, the orbital semimajor axis, and (if it is not to be considered as a system-wide constant) the mixing length for the second star. There are, however, many more observables for a binary than for a single star. Besides frequency separations for the companion, one can measure its magnitude and color, and several quantities relating to the binary's orbit. With more observables than parameters, one may reasonably fit a model to the observables, with the expectation that most (or perhaps all) of the model parameters may be well constrained. One must be careful, however, since the various pieces of information provided by the observations are unlikely to be completely independent of one another. This lack of independence has both good and bad aspects. To the extent that interdependence of the observables limits one's ability to estimate model parameters, it is obviously bad. On the other hand, if more than one observable relates to the same model parameter, then the degree of agreement between them carries information about the reliability of the data, or about genuine failings in the model that relates parameters to observables. In the most interesting case, one might hope that clearly inconsistent observables relating to the same parameter might indicate some new physics that should be included in the model.

An obvious candidate for studies of this nature is the α Centauri system, whose distance and masses are known with comparatively high precision. Furthermore, tentative identifications of p-mode oscillations have been made in the component α Cen A (Gelly et al. 1986; Pottasch et al. 1992), although other studies have failed to detect a significant signal (Brown & Gilliland 1990). Demarque, Guenther, & van Altena (1986) and Edmonds et al. (1992) attempted to model the observed properties of the system and made a preliminary investigation of the sensitivity of the frequencies to the parameters and physics characterizing the model.

In what follows, we discuss both aspects of stellar model fitting in visual binary systems, using as data the p-mode frequency separations or individual frequencies as well as reasonable photometric and astrometric observations. In § 2, we discuss the fitting procedure used and its mathematical background. Section 3 contains an example of the fitting procedure applied to a simple physical system. In § 4 we discuss the errors that we assumed for the various observables, and we describe the stellar evolution and oscillation codes used to relate model parameters to observables; this includes a careful investigation of the sensitivity of various aspects of the models and frequencies to changes in the parameters or physics. Section 5 contains the results of our numerical experiments. These were all concerned with a binary system fashioned after the α Centauri system, except at an arbitrary distance from the Earth. Section 6 is a summary of our conclusions.

2. MATHEMATICAL BACKGROUND

As a general approach to estimating stellar model parameters, we wish to employ a χ^2 minimization technique. To do so, one must first determine which observed quantities (henceforth termed *observables*) are to be used, along with the magnitudes of their associated errors. In general, it is best to use all of the pertinent observations, with the condition that the errors associated with the various observables must be independent of one another and must be reasonbly well known. The requirement of independent errors discourages use of derived quantities as observables (e.g., photometrically determined effective temperature and metallicity), since the combination of directly observed quantities (in this case photometric colors) generally leads to correlated errors in the derived values. In such cases, one should use as observables the fundamental observed quantities, which may usually be taken to have independent errors. Sometimes (for example, for parallaxes and other astrometric quantities) the line between funda-

mental observations and derived quantities is not easy or convenient to draw. These observables should be treated with care, since the introduction of correlated errors can vitiate the results of the following analysis. For the binary star systems we are considering, the observables consist of the various distinct indices obtained from astrometry, photometry, spectroscopy, and oscillation measurements. Let us suppose that there are M of these observables, designated B_i, and that each has associated with it an uncertainty σ_i.

Having chosen a set of observables, one must next construct a model of the binary system, containing a number N of free parameters P_j. The model must be such as to allow computation of all of the observables B_i, given definite values for the parameters P_j. In the present case, this model involves a sequence of rather complicated computations which will be described in detail in § 4. For the moment, it suffices to know that the model is based on stellar evolution and oscillation calculations, as well as on some information about radiative transfer, Kepler's laws, and simple geometry. It is thus able to start from a set of parameters (stellar mass, composition, distance, etc.) and produce values for the observables (magnitudes, colors, oscillation frequencies, etc.).

Although the observables are strongly nonlinear functions of the parameters, we assume that the model may be linearized in the neighborhood of a reference set of parameters P_{j0}, which are chosen to be a good first guess at the true parameter set. Then we have

$$B_i = B_{i0} + \sum_{j=1}^{N} \frac{\partial B_i}{\partial P_j} \delta P_j , \tag{3}$$

where B_{i0} is the set of observables resulting from the parameters P_{j0}, $\delta P_j \equiv P_j - P_{j0}$, and the derivatives $\partial B_i/\partial P_j$ are evaluated at $P_j = P_{j0}$. If we denote the actual values of the observables by β_i, then the parameter-fitting problem we wish to solve consists of choosing the parameter corrections δP_j so as to minimize

$$\chi^2 = \sum_{i=1}^{M} \frac{(B_i - \beta_i)^2}{\sigma_i^2} . \tag{4}$$

Within the regime where the linearization in equation (3) of the model is accurate, this is a linear least-squares problem, which is most conveniently solved by the method of singular value decomposition.

Before discussing the solution method, however, two points should be made. First, the principal purpose of this paper is to understand the uncertainties in the estimated parameter values resulting solely from errors in the observables, taken in the context of the given model. Another whole class of errors arise from inadequacies of the model itself. For example, incorrect treatment of the microphysics in the stellar evolution part of the model may lead to systematically incorrect relations between the model parameters and the observables. These errors are clearly also important; indeed, uncovering them is one of the main motivations for undertaking the modeling enterprise. In the context of the fit in equation (4), errors of this nature would appear as residuals that are inconsistent in magnitude with estimates of the errors in the data, or that are obviously systematic. We consider examples of this in § 5.6 below. However, throughout most of the paper we shall suppose that the model is adequate to reproduce the observed data, and that there is a reasonably straightforward (albeit not completely known) mapping between model parameters and the real-world quantities that they are supposed to represent. In this sense, we are discussing only the accuracy of a parameter-fitting procedure, without being concerned at present with that procedure's physical relevance.

The second point, implied by the foregoing discussion, is that it is extremely important to maintain the distinction between parameters and observables. This can be difficult to do when a parameter and an observable are related to one another in a trivial way, and therefore have similar names. For example, a stellar model requires a metal abundance Z, while spectroscopic observations can yield a stellar metallicity $Z_{\rm obs}$; in the absence of observational error, one expects that $Z_{\rm obs} = Z$. Nevertheless, these two objects are not the same, either conceptually or (very probably) numerically. They occupy different spaces and play quite different roles in the analysis.

To approach the minimization problem at hand, we will follow the discussion by Press et al. (1986). The derivative matrix $\partial B_i/\partial P_j$ describes a linear transformation relating small changes in the parameters to resulting changes in the observables. Note that to obtain a well-posed problem, we must have at least as many observables as parameters (i.e., $M \geq N$). If there are more observables than parameters, then the range of the linear transformation does not span the entire space of observables, so that in general it is not possible to fit all of the observables exactly. It is convenient to rewrite the transformation so that the change in each observable is expressed in terms of its expected error σ_i. Doing so, equation (3) becomes

$$\sum_{j=1}^{N} \frac{1}{\sigma_i} \frac{\partial B_i}{\partial P_j} \delta P_j = \delta B_i , \tag{5}$$

where $\delta B_i = (\beta_i - B_{i0})/\sigma_i$. The linear transformation may now be expressed in more compact matrix form as

$$\boldsymbol{D}\,\delta\boldsymbol{P} = \delta\boldsymbol{B} , \tag{6}$$

where $\boldsymbol{D}$ is the so-called *design matrix*, the components of which are $\sigma_i^{-1}\,\partial B_i/\partial P_j$. The χ^2 minimization problem consists of choosing $\delta\boldsymbol{P}$ so that

$$\chi^2 = \| \boldsymbol{D}\,\delta\boldsymbol{P} - \delta\boldsymbol{B} \|^2 \tag{7}$$

is a minimum.

The solution of this minimization problem by singular value decomposition hinges on the fact that $\boldsymbol{D}$ (or any other $M \times N$ matrix) may be decomposed as

$$\boldsymbol{D} = \boldsymbol{U}\boldsymbol{W}\boldsymbol{V}^T , \tag{8}$$

where $\boldsymbol{U} = \{\boldsymbol{U}^{(1)}, \boldsymbol{U}^{(2)}, \ldots, \boldsymbol{U}^{(N)}\}$ is an $M \times N$ matrix whose columns $\boldsymbol{U}^{(i)}$ are orthonormal, $\boldsymbol{W}$ is an $N \times N$ diagonal matrix, and $\boldsymbol{V} = \{\boldsymbol{V}^{(1)}, \boldsymbol{V}^{(2)}, \ldots, \boldsymbol{V}^{(N)}\}$ is an $N \times N$ matrix whose columns $\boldsymbol{V}^{(i)}$ are orthonormal. One may think of the columns of $\boldsymbol{V}$ as a set of orthonormal vectors that span the space of model parameters. The $\boldsymbol{U}^{(i)}$ are then another set of orthonormal vectors spanning the range of the transformation in observable space. Thus, no vector $\delta\boldsymbol{B}$ that is orthogonal to all the $\boldsymbol{U}^{(i)}$ can be generated by the transformation, no matter what one chooses for $\delta\boldsymbol{P}$.

For a scaled change $\delta\boldsymbol{B}$ in the observables such that equation (6) is satisfied, one obtains, using equation (8) to expand the design matrix in equation (6), and then multiplying from the left by $\boldsymbol{V}\boldsymbol{W}^{-1}\boldsymbol{U}^T$, that

$$\delta\boldsymbol{P} = \boldsymbol{V}\boldsymbol{W}^{-1}\boldsymbol{U}^T\,\delta\boldsymbol{B} . \tag{9}$$

For a general $\delta\boldsymbol{B}$ we can still obtain $\delta\boldsymbol{P}$ from equation (9). Inserting this expression into equation (7) and carrying out the

matrix multiplications, we find

$$\chi^2 = \| (1 - UU^T)\delta B \|^2 . \quad (10)$$

But because of the orthogonality of U and its identification with the range of the transformation, $(1 - UU^T)\delta B$ is precisely that component of δB that lies outside the range. The length of this residual vector therefore cannot be reduced by any other choice of δP, so that the vector δP in equation (9) is in fact the desired minimum χ^2 solution. This may be expressed as $\delta P = Q\,\delta B$, where the matrix

$$Q = VW^{-1}U^T \quad (11)$$

determines the weight given to each datum in the determination of an individual parameter P_j. Having so determined the solution δP, we may compute the residual vector

$$\delta B_{\rm resid} = \delta B - D\,\delta P; \quad (12)$$

as discussed above, large components of $\delta B_{\rm resid}$ (i.e., given our normalization with the errors, components substantially larger than unity) indicate that the data are inconsistent with the assumed model.

Besides it elegance, the singular value decomposition (SVD) method for obtaining a best fit to the observables has several practical advantages. The most important of these concerns the errors that should be associated with the parameter estimates. Because of the presumed independence of the errors in the observables and the division by σ_i, the error ellipsoid in the space of δB is in fact a sphere. Following the transformation to parameter space, the error ellipsoid surrounding δP is generally not spherical at all, and moreover its principal axes need not be aligned with the coordinate axes. A major convenience of the SVD method is that the columns of V are precisely the principal axes of the error ellipsoid, while the corresponding (diagonal) values of W^{-1} are the lengths of these axes. To see this, assume for simplicity that the expectation values of δB and δP are zero. Then the error ellipsoid is defined by a constant value of

$$\| \delta B \|^2 = \| WV^T \delta P \|^2 = \sum_{i=1}^{N} W_{ii}^2 [V^{(i)} \cdot \delta P]^2 , \quad (13)$$

where equations (6) and (8) were used. Here the bold face dot denotes scalar product between vectors in parameter space; hence $| V^{(i)} \cdot \delta P |$ is the magnitude of the component of δP along $V^{(i)}$. Equation (13) clearly defines the error properties in terms of principal axes in parameter space. One may thus determine by inspection which combinations of parameters are well or poorly determined.

Another useful representation of the errors is the error covariance matrix C, which is given by

$$C_{jk} \equiv \langle \Delta P_j \Delta P_k \rangle = \sum_{i=1}^{N} \frac{V_{ji} V_{ki}}{W_{ii}^2} , \quad (14)$$

where the ΔP_j are the errors in parameter estimates resulting from errors in the observed quantities, and angle brackets denote expectation value. The diagonal elements of C correspond to the squared error expected in each of the parameters, without concern for the (possibly correlated) errors in other parameters. These diagonal elements thus convey the total range of variation that one may expect for each parameter, but if the off-diagonal elements of C are large, they may not accurately represent the power of the observables to constrain the solution. A more helpful measure in such cases may be the volume of the error ellipsoid (i.e., the volume of parameter space in which the correct solution is likely to lie), which is proportional to the product of the diagonal elements of W^{-1}. It should be noted, however, that because the axes of the error ellipsoid need not align with the parameter axes, this measure is not always useful in estimating the probable range of variation in a given parameter. This situation is illustrated in Figure 1, which shows a case in which improved measurement precision in one observable (solid vs. dashed error ellipses) leads to a substantial decrease in the volume of the error ellipse in parameter space, without noticeably decreasing the rms error of either parameter taken alone. In the following, we generally use as a measure of precision the rms error associated with each parameter taken alone, rather than the volume of the error ellipsoid, since the individual parameters are of greater physical interest.

Another convenient aspect of the SVD method is that one may easily determine which observables are important in determining each of the orthogonal components (given by the columns of V) of the solution. To each column $V^{(i)}$ of V corresponds the column $U^{(i)}$of U; the importance of observable j in determining that component of the solution is proportional to the magnitude of the jth element U_{ji} in $U^{(i)}$. If observable j does not have a large component in any of the vectors $U^{(i)}$, then it is not important in determining any aspect of the solution and may be considered superfluous. The importance of an observable may be considered inversely proportional to the change in that observable (measured in units of its expected error) that is required to move the solution in parameter space from the center to the surface of the error ellipsoid (see Fig. 1*b*). This can be made more precise by noting that according to equation (13) the location in the error ellipsoid corresponding to a given realization δB of the observables (assuming again zero expectation values) is given by

$$\| WV^T \delta P \|^2 = \| U^T \delta B \|^2 . \quad (15)$$

If δB has only one nonzero component, δB_j, this expression is equal to $S_j^2\,\delta B_j^2$, where

$$S_j = \left(\sum_{i=1}^{N} U_{ji}^2 \right)^{1/2} \quad (16)$$

is a measure of significance of the jth observable. Because of the orthonormal property of the columns of U, S_j may range between zero (for totally irrelevant observables) to unity (for the most important ones).

3. A SIMPLE EXAMPLE

To illustrate some of the properties of the technique discussed in the preceding section, we consider a simple example of an overdetermined observed system: the apparent intensity of a blackbody, characterized by temperature and emissivity, and observed at three wavelengths. The intensity at wavelength λ can be written as

$$I(\lambda) = E\lambda^{-5} \exp\left(-\frac{c_1}{\lambda T} \right) , \quad (17)$$

where E is the emissivity and T the temperature; we take as the two parameters P_j to be determined $P_1 = \log E$ and $P_2 = \log T$. We assume that the intensity is measured at three wavelengths λ_i, $i = 1, 2, 3$, to give the observables $B_i = \log I(\lambda_i)$, $i = 1, 2, 3$. As in the general case we linearize the model around a reference set of parameters ($\log E_0$, $\log T_0$), with corresponding observables $\log I_0(\lambda_i)$. The errors are supposed to be uniform; without loss of generality we take them to be unity.

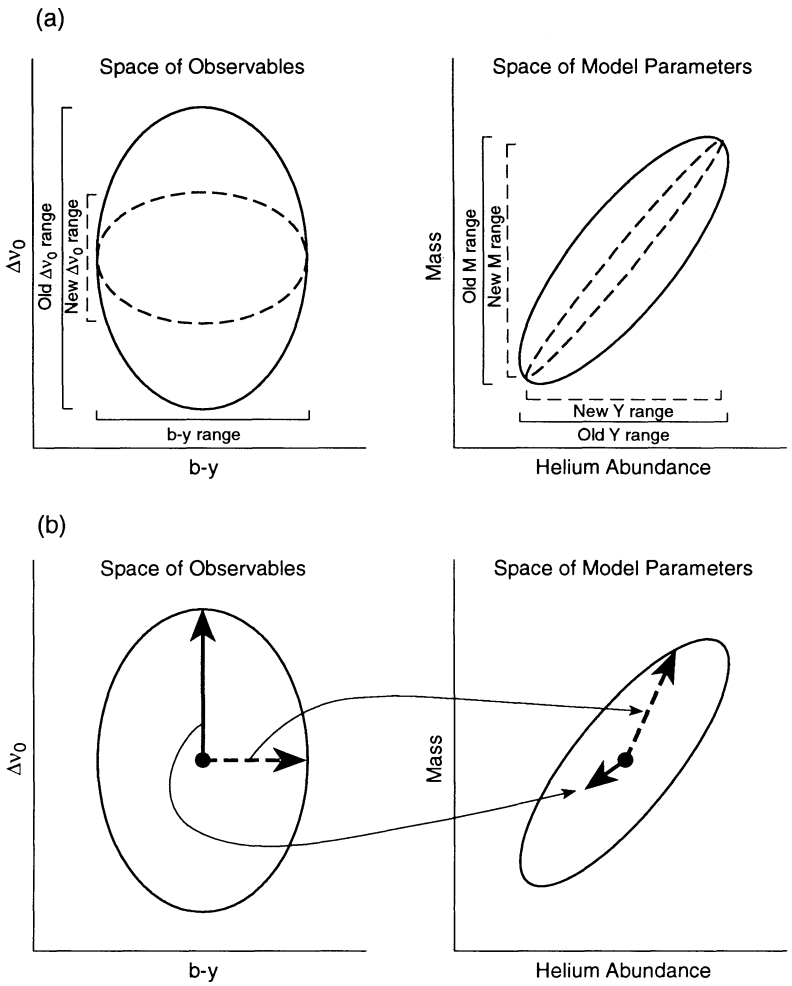

FIG. 1.—Illustration of aspects of the transformation between observables (*left*) and parameters (*right*). (*a*) Shrinking the error ellipsoid in one dimension in observable space (solid vs. dashed ellipse) may result in a corresponding reduction of the volume of the ellipsoid in parameter space, without substantially changing the range of variation of any parameter. (*b*) The effect of significant ($b - y$, in this case) and insignificant (Δv_0) observables on the inferred parameters. A change of 1 σ in $b - y$ (*dashed arrow*) causes the solution vector to move almost to the 1 σ probability contour in parameter space. A 1 σ change in Δv_0 (*solid arrow*), however, moves the solution vector only a fraction as far. In this case, $b - y$ is much more significant than Δv_0.

For this model, the transformation is given by equation (6), with a derivative (or design) matrix $\boldsymbol{D}$ determined by

$$\left.\begin{aligned} \frac{\partial B_i}{\partial P_1} &= 1 \,, \\ \frac{\partial B_i}{\partial P_2} &= \frac{y_i}{1 - \exp\,(-y_i)} \,, \end{aligned}\right\} \quad i = 1, 2, 3 \,, \tag{18}$$

where $y_i = c_1/(\lambda_i T_0)$. Hence the properties of the problem are characterized by the values of y_i.

We consider the case $\{y_i\} = (6, 8, 10)$, essentially corresponding to the region of validity of Wien's approximation to the blackbody curve; accordingly, $\partial B_i/\partial P_2 \simeq y_i$. Here the analysis yields

$$\boldsymbol{U} = \begin{Bmatrix} -0.806 & -0.427 \\ -0.115 & -0.566 \\ 0.581 & -0.707 \end{Bmatrix}, \quad \boldsymbol{V} = \begin{Bmatrix} -0.993 & -0.119 \\ 0.119 & -0.993 \end{Bmatrix},$$

$$\boldsymbol{C} = \begin{Bmatrix} 8.40 & -1.00 \\ -1.00 & 0.126 \end{Bmatrix}. \tag{19}$$

The singular values are 0.343 and 14.25. Hence the small singular value is associated with the first column of $\boldsymbol{V}$ which principally contributes to log E, whereas the second column of $\boldsymbol{V}$, which is dominated by log T, corresponds to the large singular value. This is also reflected in the diagonal elements of the covariance matrix C, which shows that the error in log E (with the assumed unit error in the observables) is 2.9, whereas the error in log T is only 0.35. It is hardly surprising that log T is substantially better determined than log E, in view of the fact that a given change in log T produces a substantially larger change in the observables than does the same change in log E.

It is interesting to consider how the data are combined to determine the individual parameters P_j. This is determined by the matrix $\boldsymbol{Q}$ given in equation (11). For the case considered above

$$\boldsymbol{Q} = \begin{Bmatrix} 2.340 & 0.337 & -1.677 \\ -0.251 & 0.000 & 0.251 \end{Bmatrix}. \tag{20}$$

This shows in particular that log T is determined almost entirely by the difference between log $I(\lambda_1)$ and log $I(\lambda_3)$: indeed, this corresponds simply to the color index which is

what one would naively have used to measure the temperature. The determination of log E, on the other hand, relies on a more complicated combination of observables.

For comparison, we consider also the case where the wavelengths of the observations are widely separated, by taking $\{y_i\} = (0.5, 6, 10)$. In particular, there is now a point on the red side of the maximum in the blackbody curve. The resulting expansion matrices are

$$\boldsymbol{U} = \begin{Bmatrix} 0.921 & 0.117 \\ 0.264 & 0.515 \\ -0.287 & 0.849 \end{Bmatrix}, \quad \boldsymbol{V} = \begin{Bmatrix} 0.992 & 0.125 \\ -0.125 & 0.992 \end{Bmatrix},$$

$$\boldsymbol{C} = \begin{Bmatrix} 1.202 & -0.151 \\ -0.151 & 0.0262 \end{Bmatrix}, \tag{21}$$

with singular values 0.905 and 11.83. Although it is still the case that log T is better determined than log E, the error in the latter has been reduced considerably, to 1.1, whereas the error in log T is now 0.16. The weights in determining the parameters are given by

$$\boldsymbol{Q} = \begin{Bmatrix} 1.011 & 0.295 & -0.306 \\ -0.118 & 0.007 & 0.111 \end{Bmatrix}; \tag{22}$$

hence again log T is predominantly determined by the color index corresponding to the extreme wavelengths, although with a small contribution from the intensity at the intermediate wavelength.

If the observed intensities do not follow the Planck law, then in general the derived values of emissivity and temperature will be incorrect, and moreover the intensities corresponding to the derived parameter values will not exactly match the observed ones. As an example, suppose that the intensity at the intermediate wavelength were to increase by 1 unit, perhaps due to some narrow-band emission process. Thus, $\delta\boldsymbol{B} = \{0, 1, 0\}$. From equation (22), the resulting estimates of log E and log T would increase by 0.295 and 0.007, respectively. These changes would not suffice to reproduce the observed intensities, however. Residuals in the observed intensities would remain, given by equation (12). In the current case, these would be $\delta\boldsymbol{B}_{\rm resid} = \{-0.303, 0.665, -0.361\}$, which are evidently of approximately the same size as the imposed intensity perturbation. Had the hypothetical emission process instead perturbed the intensity at one of the extreme wavelengths, the inferred changes in log E and log T would have been larger, and the residual intensities would have been smaller by a factor of about 2. This illustrates an obvious point, namely that the detectability of a new physical effect depends upon how closely its consequences resemble those of the processes already assumed to be operating.

4. NUMERICAL MODELS

4.1. *Observables and Their Errors*

To allow definition of a model binary star system, we compiled a list of observables (including oscillation parameters) that should be accessible for a well-observed system. This list is by no means exhaustive, but does nonetheless capture most of the available information about the evolutionary state of such a system. A list of the observables, including their standard errors, defining our reference case is given in Table 1. However, we also consider cases where additional variables were included in the fit, particularly individual frequencies, or where

TABLE 1

OBSERVABLES AND STANDARD ERRORS

Observable	σ
m_{yA}	0.005 mag
$(b-y)_A$	0.005 mag
log Z	0.17
π'	0.″004
$(\Delta\nu_0)_A$	0.06 μHz
$(\delta\nu_0)_A$	0.82 μHz
m_{yB}	0.005 mag
a'	0.″05
$(b-y)_B$	0.005 mag
log (M_A/M_B)	0.004
log $P_{\rm orbit}$	0.0001
$(\Delta\nu_0)_B$	0.06 μHz
$(\delta\nu_0)_B$	0.82 μHz

NOTES.—Data for field star (top section), and for visual binary (both sections combined). The values of σ define our reference case. In some of our experiments the separations $\Delta\nu_0$ and $\delta\nu_0$ were replaced by frequencies of invidual modes, assumed to be determined with a standard error of 2 μHz.

the standard errors on some of the observables are reduced, or increased. Insofar as possible, the scales and units used for the observables (linear or logarithmic scales, linear or angular measure, etc.) were chosen so that the errors are independent of the value of the thing being measured, the distance to the binary, or the physical parameters of the system. This was not always possible, as for instance in the case of the orbital period $P_{\rm orbit}$, the error of which depends on a great many factors, including how long the system has been observed. In this and similar cases, we used values appropriate to the real α Cen system. Since the observations of α Cen are so good, this practice tends to minimize the importance of new information, such as oscillation data.

Some of the observables require further comment. Stellar magnitudes m_y and colors $(b-y)$ are both assumed to have typical errors of 0.005 mag, or 0.5%. This is perhaps a reasonable estimate of the accuracy with which magnitudes and colors may be reduced to a standard photometric system, even though measurement repeatability with a single instrument may be better than this. There is only one color observable $(b-y)$ for each star, because we felt that the information carried by other colors concerning, for example, surface gravity or metallicity would be superseded by other kinds of observation. The error assumed for log $Z_{\rm obs}$ ($Z_{\rm obs}$ being the observed heavy-element abundance) is based on recent detailed spectroscopic studies (e.g., Edvardsson et al. 1993) and is comparable also with the best current measurements for α Cen itself (Furenlid & Meylan 1990). The error in parallax π' of 0.″004 is typical of the best current ground-based measurements (Kamper & Wesselink 1978; Flannery & Ayres 1978); the *HIPPARCOS* mission is expected to provide parallaxes for a large sample of stars that are more accurate than this by a factor of about 2 (Gómez 1993). The apparent semimajor axis a', mass ratio M_A/M_B, and orbital period $P_{\rm orbit}$ are all assumed to be determined to very high precision through astrometric observations. The values used in the table are typical of the errors quoted for the very best observed visual binaries, such as α Cen itself. For stars that are significantly farther away (so that the apparent separation is smaller), or that have longer periods, or that have not been so thoroughly observed, the errors would increase dramatically.

Since solar-like oscillations have not yet been definitely identified on other stars, it is difficult to estimate their errors accurately. We have assumed that individual frequencies can be determined with rms errors of 2 μHz; this is representative of current solar observations lasting for about a week. To estimate the magnitude of α for the large and small frequency separations in the reference case, we have assumed that one-half of the modes with $0 \leq l \leq 3$ and $17 \leq n + l/2 \leq 29$ have large enough amplitudes during a given observing run so that their frequencies can be measured. The error estimates of 0.06 μHz for $\Delta\nu_0$ and 0.82 μHz for $\delta\nu_0$ then follow from a least-squares fit of the mode frequencies to the asymptotic frequency relation. $\Delta\nu_0$ is much better determined than $\delta\nu_0$, because the frequency spacing between modes with the smallest and largest n-values is proportional to n, as well as to $\Delta\nu_0$. To evaluate the information content in the oscillation frequencies we have considered two different cases: in one, we assume that the oscillation frequencies can be adequately expressed in terms of only the two parameters $\Delta\nu_0$ and $\delta\nu_0$; in the second case, we include individual mode frequencies in the analysis. The latter type of experiment clearly serves to illustrate the potential loss of information resulting from representing the frequencies in terms of a small set of parameters derived from a fit based on the expected asymptotic behavior. In our reference case we assume that oscillation measurements are available for both stars in a binary system; however, we also consider the effect of having frequency data for only the brighter star of the pair. For cases in which we wished to assume that no oscillation frequencies were available, we set the corresponding errors to 10^5 μHz. These data are then given negligible weight in determining the least-squares solution.

In some cases (those concerning isolated field stars with no oscillation information), there are fewer well-determined observables than model parameters. In these underconstrained cases, we have restricted the parameter error estimates to reasonable ranges by adding pseudo-observables, consisting of the values of log M, log Y, log Z, and log τ. These pseudo-observables (prejudices, really) are assigned σ values that represent the entire plausible range of the corresponding parameter for a randomly chosen star of roughly solar type. By using these prejudices as data, one arrives at parameter estimates that do not conflict with common astrophysical understanding, and in which the genuine observables may play some role in improving the solution. It should be clearly understood, however, that at least some aspects of the error estimates in these cases reflect nothing more than the built-in bias. The pseudo-observables and their assumed 1 σ errors are shown in Table 2.

TABLE 2

PREJUDICES FOR FIELD STARS

Pseudo-Observable	σ
log M_A	0.20
log Y	0.12
log α	0.40
log τ	1.20

NOTE.—Values applied to stabilize results of error estimation for the field-star case without oscillation information.

4.2. *Computation of Stellar Evolution Models and Frequencies*

In the general binary star case the model that generates the observables and their derivatives has nine free parameters. They are listed in Table 3, along with their assumed values; these were chosen to obtain a pair of models similar to α Cen A and B, although no attempt was made to match the observed properties closely. To facilitate comparisons between errors in the different parameters, we express all of these as errors in the logarithm of the parameter (i.e., proportional to relative errors). The most substantial part of the model consists of a stellar evolution code, which takes as input the mass of each component (M_A, M_B), the initial composition of the system (Y, Z), the age τ of the system, and the convective mixing-length parameters α_A, α_B (which in general are assumed to be different for the two stars). Note that τ is specified in years, rather than in fractions of an evolutionary timescale, since it is important that both stars have the same age, not the same evolutionary state.

The reference stellar models were computed with the parameters listed in Table 3, by means of a "standard" evolution calculation. This largely followed the procedures described by Christensen-Dalsgaard (1982). The Eggleton, Faulkner, & Flannery (1972) equation of state was used, together with opacities determined from the Los Alamos Opacity Library (Heubner et al. 1977) by Courtaud et al. (1990), using the Anders & Grevesse (1989) heavy-element abundances with the then assumed photospheric iron abundance. The nuclear reaction parameters were obtained largely from Parker (1986); the abundance of ^{3}He was assumed to be in nuclear equilibrium, as was the CNO cycle.

We determined oscillation frequencies for the models by solving the equations of adiabatic oscillation (see Christensen-Dalsgaard & Berthomieu 1991 for further detail). To obtain measures of the average separations $\Delta\nu_0$ and $\delta\nu_0$ we used a least-squares fit to the computed frequencies, based on the asymptotic properties of low-degree modes, as described by Christensen-Dalsgaard (1988). In the reference case the fit included modes of degree $l = 0$–3 and with $17 \leq n + l/2 \leq 29$.

Properties of the computed reference models are listed in the first column of Table 4. (The remaining columns refer to models where the physics has been modified; these models are discussed in § 5.6 below.) To provide an indication of the internal structure of the stars, we have included the central hydrogen abundance, temperatures, and density, as well as the depths of the outer convection zone, even though these quantities evidently do not enter directly into the evaluation of our observables. Also included are the large and small frequency separations.

TABLE 3

PARAMETERS OF THE MODEL

Model Parameter	Value(s)
log M_A	0.0374
log Y	−0.5510
log Z	−1.7000
log α_A	0.4007
log τ	9.544
log D	0.114, 1., 2.
log M_B	−0.0458
log α_B	0.4007
log a	1.301

NOTES.—Data for field star (top section), and for visual binary (both sections combined). Masses are in units of the solar mass, age in yr, distance in pc, semimajor axis in AU.

TABLE 4

PROPERTIES OF MODELS

PHYSICS	CASE I Reference	CASE II CEFF	CASE III OPAL	CASE IV OPAL[a]	CASE V OPAL,[a] diff.
			Model A		
$L/L_\odot$	1.509	1.616	1.458	1.443	1.458
$T_{\rm eff}$ (K)	6039.	6073.	6202.	5988.	5956.
$R/R_\odot$	1.124	1.151	1.048	1.119	1.136
X_c	0.2971	0.2648	0.3135	0.3174	0.3021
T_c (10^6 K)	16.96	17.36	16.69	16.65	16.78
ρ_c (g cm^{-3})	156.3	165.0	154.9	153.9	158.5
d_b/R	0.2208	0.2124	0.2663	0.2385	0.2489
$\Delta\nu_0$ (μHz)	118.7	114.9	132.1	120.5	117.9
$\delta\nu_0$ (μHz)	8.748	8.430	9.066	8.778	8.514
			Model B		
$L/L_\odot$	0.5037	0.5415	0.4950	0.4828	0.4878
$T_{\rm eff}$ (K)	5335.	5393.	5458.	5313.	5299.
$R/R_\odot$	0.8323	0.8446	0.7882	0.8217	0.8303
X_c	0.5272	0.5161	0.5308	0.5337	0.5192
T_c (10^6 K)	13.18	13.40	13.10	13.03	13.10
ρ_c (g cm^{-3})	104.2	107.0	103.9	103.2	105.7
d_b/R	0.3010	0.2969	0.3151	0.3073	0.3120
$\Delta\nu_0$ (μHz)	168.4	165.2	182.7	180.1	169.7
$\delta\nu_0$ (μHz)	12.31	12.13	12.63	12.45	12.18

NOTES.—The models are distinguished by the physics (see text). Variables that have not previously been defined have the following meaning: X_c, T_c, and ρ_c are the central hydrogen abundance, temperature, and density, and d_b is the depth of the outer convection zone. Model A refers to the 1.09 $M_\odot$ model and model B refers to the 0.9 $M_\odot$ model.

[a] Mixing length has been obtained from calibrating a model of the present Sun with the OPAL opacities.

To compute derivatives involving the model and oscillation calculations, we varied each of the parameters M_A, M_B, Y, Z, α_A, α_B, and τ separately, by suitable small amounts. Each derivative was computed from differences centered on the reference values given in Table 3. The actual increments used were 0.005 $M_\odot$ for M_A and M_B, 0.005 for Y, 0.001 for Z, 0.1 for α_A and α_B and 2.5×10^8 yr for the ages. We tested that the increments were large enough that numerical problems were avoided, yet small enough that the assumed linearity was satisfied with adequate precision. The resulting derivatives, for all the quantities given in Table 4, are presented in Table 5. To illustrate the extent to which the frequency derivatives result from the approximate proportionality of frequency with the mean density (cf. eq. [1]), we also show derivatives of $3/2 \ln R + \ln \Delta\nu_0$ and $3/2 \ln R + \ln \delta\nu_0$. This shows that for $\Delta\nu_0$ the variation is almost entirely related to the variation in $MR^{-3/2}$; for $\delta\nu_0$, on the other hand, there remains a substantial effect, although the dependence of $\delta\nu_0$ on composition is evidently to a large extent a radius effect.

Individual derivatives of the frequencies, after correcting for the effect of $\bar{\rho}$, are shown in Figure 2. Except for the derivatives with respect to the age τ, the dominant trend is that the derivatives depend little on degree and display a smooth variation with frequency. This behavior indicates that the dominant source of the frequency change is very near the stellar surface (e.g., Christensen-Dalsgaard & Berthomieu 1991). Such parameter sensitivity would be difficult to disentangle from the uncertainties in the treatment of the physics of the outermost layers, where nonadiabaticity and dynamical effects of convection have to be taken into account. Furthermore, the derivatives

TABLE 5

DERIVATIVES OF STELLAR MODEL RESULTS

Parameter	$\ln M$	$\ln Y$	$\ln Z$	$\ln \tau$	$\ln \alpha$
			Model A		
$\ln L$	6.03	2.38	−0.80	0.37	0.018
$\ln T_{\rm eff}$	0.54	0.27	−0.10	0.012	0.11
$\ln R$	1.94	0.64	−0.19	0.16	−0.20
$\ln X_c$	−7.54	−4.59	0.88	−1.63	−0.026
$\ln T_c$	1.70	0.90	−0.19	0.21	0.005
$\ln \rho_c$	3.45	2.26	−0.64	0.87	0.012
$\ln d_b/R$	−3.11	−1.49	0.76	−0.026	0.54
$\ln \Delta\nu_0$	−2.39	−0.96	0.29	−0.23	0.29
$\ln \delta\nu_0$	−2.72	−1.15	0.27	−0.59	0.11
$3/2 \ln R + \ln \Delta\nu_0$	0.52	0.006	0.005	0.008	−0.012
$3/2 \ln R + \ln \delta\nu_0$	0.19	−0.18	−0.019	−0.35	−0.19
			Model B		
$\ln L$	5.39	2.06	−0.67	0.17	0.062
$\ln T_{\rm eff}$	0.74	0.38	−0.12	0.019	0.081
$\ln R$	1.22	0.26	−0.10	0.046	−0.13
$\ln X_c$	−1.26	−1.11	0.15	−0.33	−0.014
$\ln T_c$	1.07	0.58	−0.11	0.073	0.012
$\ln \rho_c$	1.37	1.17	−0.35	0.30	0.016
$\ln d_b/R$	−0.69	−0.33	0.23	0.011	0.095
$\ln \Delta\nu_0$	−1.30	−0.39	0.16	−0.067	0.19
$\ln \delta\nu_0$	−1.06	−0.27	0.063	−0.22	0.065
$3/2 \ln R + \ln \Delta\nu_0$	0.52	0.001	−0.001	0.002	−0.010
$3/2 \ln R + \ln \delta\nu_0$	0.76	0.12	−0.094	−0.15	−0.13

NOTES.—Logarithmic derivatives of various properties of the computed models, with respect to the model parameters. Model A refers to the 1.09 $M_\odot$ model and model B refers to the 0.9 $M_\odot$ model. Variables have been defined in the notes to Table 4.

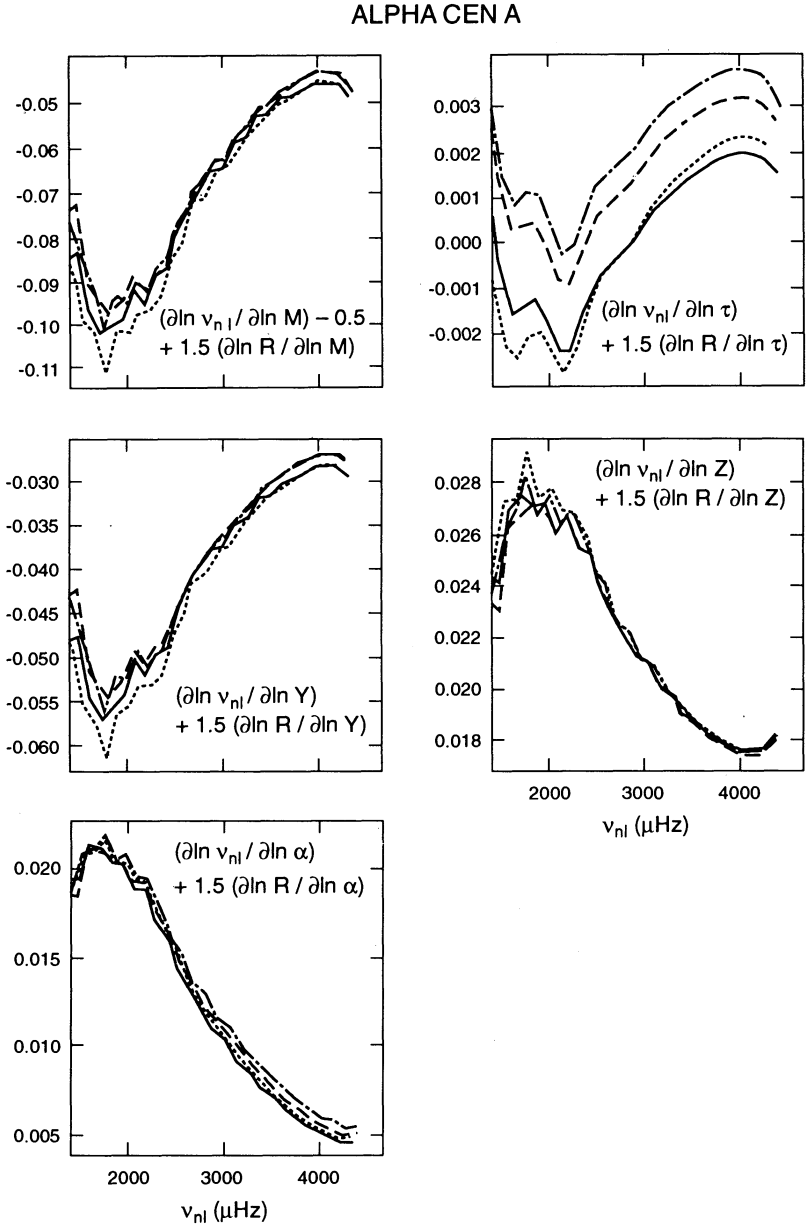

FIG. 2.—The variation with parameter value of $\ln \nu_{nl}$ for p modes in the α Cen A reference case, shown as a function of mode frequency. These frequency shifts have been corrected for changes in mean density that accompany the parameter changes and constitute the dominant source of frequency changes. Different line styles indicate modes with different values of angular degree l: $l = 0$ (*solid line*); $l = 1$ (*dotted line*); $l = 2$ (*dashed line*); and $l = 3$ (*dash-dotted line*). Note that only the age causes significant l-dependence in the frequency changes; other parameters cause shifts that are predominantly functions of frequency.

with respect to mass, composition, and mixing length are evidently rather similar, apart from sign and scaling, making it difficult to separate the influence of these parameters. Overlying the general trend are oscillatory components which may be related to changes in the helium ionization zone or at the base of the convection zone (e.g., Gough 1990b). In contrast, the frequency derivatives with respect to τ show a comparatively strong dependence on l; this is reflected in the $\partial \ln \delta\nu_0 / \partial \ln \tau$ showed in Table 5, and clearly underlies the potential usefulness of $\delta\nu_0$ as a measure of stellar age. It should be noted, however, that the τ-derivatives are extremely small, hence imposing stringent demands on the allowable errors in the frequencies.

4.3. *Photometric and Astrometric Variables*

For each component the evolution code provides the stellar luminosity L_*, surface gravity g_*, and effective temperature T_*, as well as the model quantities required in the subsequent calculation of the oscillation frequencies. From L_*, T_*, and g_*, we are able to use the relations in Edvardsson et al. (1993) to estimate the $b - y$ color. These combined with the distance D to the system, yield the visual magnitudes $m_{y,A}$, $m_{y,B}$, and the colors $(b - y)_A$ and $(b - y)_B$. The mass ratio M_A/M_B, the orbital period $P_{\rm orbit}$, the apparent semimajor axis a', and the apparent parallax π' are all computed directly from the stellar masses, the orbital semimajor axis a, and the distance D. The

TABLE 6

DERIVATIVE MATRIX

OBSERVABLES	MODEL PARAMETERS								
	$\log M_A$	$\log M_B$	$\log Y$	$\log Z$	$\log \tau$	$\log \alpha_A$	$\log \alpha_B$	$\log D$	$\log a$
m_{yA}	−15.1	0.	−5.94	2.41	−0.92	−0.04	0.	5.00	0.
m_{yB}	0.	−13.5	−5.14	2.05	−0.42	0.	−0.16	5.00	0.
$(b-y)_A$	−1.16	0.	−0.59	0.29	−0.03	−0.21	0.	0.	0.
$(b-y)_B$	0.	−1.38	−0.70	0.29	−0.04	0.	−0.15	0.	0.
$\log(M_A/M_B)$	1.00	−1.00	0.	0.	0.	0.	0.	0.	0.
$\log P_{\rm orbit}$	−0.27	−0.23	0.	0.	0.	0.	0.	0.	1.50
a'	0.	0.	0.	0.	0.	0.	0.	−35.4	35.4
$\log Z$	0.	0.	0.	1.00	0.	0.	0.	0.	0.
π'	0.	0.	0.	0.	0.	0.	0.	−1.77	0.
$(\Delta\nu_0)_A$	−653.	0.	−263.	98.3	−63.9	79.7	0.	0.	0.
$(\Delta\nu_0)_B$	0.	−505.	−152.	71.1	−25.9	0.	72.1	0.	0.
$(\delta\nu_0)_A$	−54.8	0.	−23.2	7.03	−11.9	2.31	0.	0.	0.
$(\delta\nu_0)_B$	0.	−30.2	−7.75	2.33	−6.11	0.	1.85	0.	0.

NOTES.—Derivative matrix $\partial B_i/\partial P_j$, relating observables to model parameters, for binary system at 1.3 pc. The parallax π' and the apparent separation a' are in arcseconds, and the frequency separations $(\Delta\nu_0)_A$, $(\Delta\nu_0)_B$, $(\delta\nu_0)_A$, and $(\delta\nu_0)_B$ are in μHz.

relations used for this purpose are

$$\log\left(\frac{M_A}{M_B}\right)_{\rm obs} = \log\left(\frac{M_A}{M_B}\right), \tag{23}$$

$$\log(P_{\rm orbit}) = \tfrac{3}{2}\log a - \tfrac{1}{2}\log(M_A + M_B), \tag{24}$$

$$a' = \frac{a}{D}, \tag{25}$$

$$\pi' = \frac{1}{D}. \tag{26}$$

Note that we do not include orbital elements other than a' and $P_{\rm orbit}$ in the list of observables, since such quantities (e.g., the orbital eccentricity) have to do only with orbital dynamics, and not with the structural parameters of the individual stars. The heavy-element abundance determined by spectroscopy is assumed to be (in the absence of observational error) the same as the corresponding model parameter:

$$Z_{\rm obs} = Z. \tag{27}$$

The photometric calibrations, together with the model derivatives given in Table 5, and the analytical relations (23)–(27) finally allow us to compute the complete set of derivatives $\partial B_i/\partial P_j$. The result is shown in Table 6, assuming a distance of 1.3 pc, for the case where frequency separations are used.

5. RESULTS

In this section we will summarize the results of performing the sensitivity analysis just described, using a wide enough range of assumed parameters to illustrate most of the effects that are likely to arise in practice.

5.1. *SVD Applied to the Reference Case*

To help estimate the usefulness of oscillation data in studying the real α Cen system, and to provide a starting point for later comparisons, we first consider a reference case that is constructed to resemble the true system fairly closely, with reasonable assumptions about the oscillation data that may soon become available. We shall first illustrate the SVD formalism as applied to this particular set of parameters and observables; later we shall return to consider the physical implications of the results.

In the reference case, we assume that the observations relate to a visual binary system in which photometric and seismological observations are available for both stars. We also assume that *p*-mode frequencies are available in the angular-degree range $0 \le l \le 3$, and that each star of the pair is described by its own mixing-length parameter. Errors for the observables and nominal values of the parameters are those given in Tables 1 and 2. Note that we consider variations in the distance to the system, as well as different levels of oscillation-frequency information (none, or frequency separations $\Delta\nu_0$ and $\delta\nu_0$ only, or complete frequency information for the modes) to correspond to different aspects of the same "reference" case.

Figure 3 shows the singular values, orthogonal parameter vectors, and corresponding combinations of observables for the reference case at distances of 1.3 and 100 pc, including the frequency separation data only. Note first that the singular values in Figure 3*a* are quite disparate in size, with almost three orders of magnitude separating the largest and the smallest. Thus some combinations of parameters are much better determined than others. The parameter combinations $\boldsymbol{V}^{(i)}$ corresponding to the different singular values are shown in Figure 3*b*, and the observable combinations $\boldsymbol{U}^{(i)}$ in Figure 3*c*. It is interesting that in this case (as in most others we have examined), most of the orthogonal parameter vectors $\boldsymbol{V}^{(i)}$ consist of rather complicated and obscure combinations of the parameters. Moreover, the set of observables $\boldsymbol{U}^{(i)}$ corresponding to the vectors $\boldsymbol{V}^{(i)}$ are also, for the most part, fairly complicated. If one wishes to understand the fitting process in intuitive terms, these complications are unfortunate. It would be convenient if one could argue (as is commonly done when fitting stellar models to data) along the following lines: "The parallax determines the distance to the system. Given the distance, the other astrometric indices determine the masses and the orbital semimajor axis. The distance and the magnitudes determine the luminosities ...." An examination of Figure 3 shows that the SVD operates very differently. The parallax, for instance, is most important in determining $\boldsymbol{V}^{(6)}$, $\boldsymbol{V}^{(7)}$, and $\boldsymbol{V}^{(8)}$, which are combinations involving almost every parameter *except* the distance. The distance appears most prominently in $\boldsymbol{V}^{(4)}$, which depends mostly on the photometric magnitudes

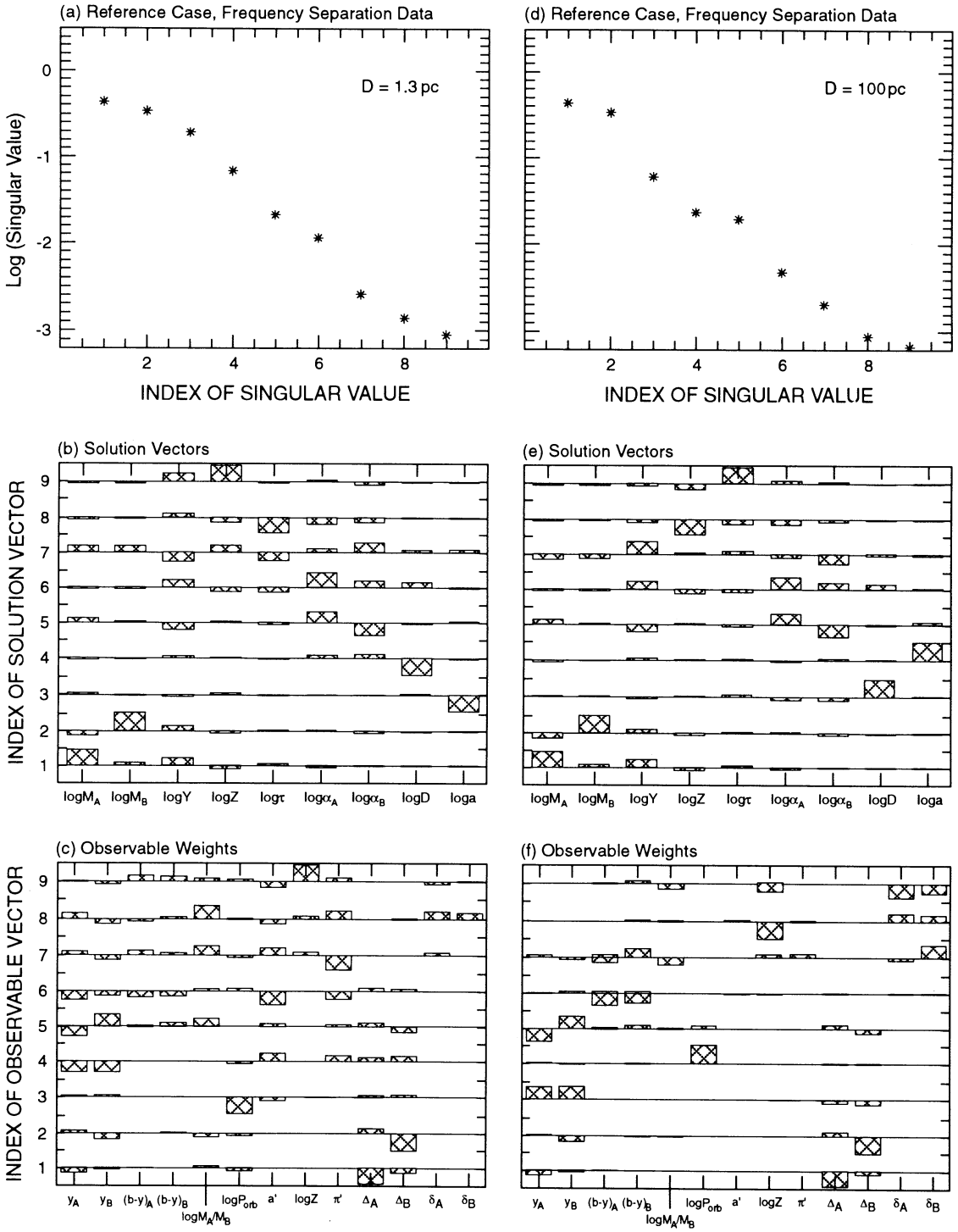

FIG. 3.—Characteristics of the SVD solution for the reference case at $D = 1.3$ pc (panels *a–c*) and $D = 100$ pc. (panels *d–f*). (*a*) Singular values (note the logarithmic scale). (*b*) Solution vectors, i.e., the vectors in parameter space corresponding to the singular values in (*a*). Components of the vectors along each parameter axis are shown as positive- or negative-going bars with lengths in the range $[-1, 1]$. Thus, the solution vector corresponding to the largest singular value has substantial positive contributions from $\log M_A$ and from $\log Y$, with lesser components from the other parameters. (*c*) Contributions of the various observables to the inferred amplitudes of the corresponding solution vectors, in the same format as (*b*). Thus, the amplitude of the first solution vector is determined mostly by Δv_{0A}, with lesser contributions from y_A and from Δv_{0B}. Panels *d–f* show similar results for $D = 100$ pc. Note the generally smaller singular values, and the rearrangement and modification of the solution and observable vectors resulting from the loss of astrometric information.

and the apparent semimajor axis, and only slightly on the parallax.

The problem with the straightforward approach is that most observables are influenced by many parameters, and hence carry at least some information about those parameters. Also, the observables vary widely in their precision and their sensitivity to changes in the various parameters. Thus, the connection between observables and parameters that is the most conceptually straightforward is often not the one that yields the most precise results. It is sometimes nonetheless possible to make fairly direct connections between the observables and the parameters, particularly when one observable is much better determined than the rest. If, for instance, one ascribes a very small error to $P_{\rm orbit}$ while leaving the other errors unchanged, then the parameter vector corresponding to the largest singular value turns out to be a combination of the masses and the semimajor axis resulting from Kepler's laws, and determined entirely by $P_{\rm orbit}$. In cases like the current one, where almost all of the observables play roles of similar importance in constraining the parameters, such simple results are uncommon.

The singular values and vectors corresponding to a distance of 100 pc are shown in Figures 3*d–f*. Relative to the 1.3 pc case, the singular values are decreased somewhat, reflecting the increase in the errors in the determination of the parameters. Also, the parallax π' and the semimajor axis a' are given much smaller weight than before in the $U^{(i)}$: with increasing distance these quantities are less effective as constraints on the solution. On the other hand, the weights on the small frequency separations $\delta\nu_{0,A}$ and $\delta\nu_{0,B}$ are substantially larger, although the influence of these observables is still confined to the smallest singular values, and hence the least well-determined components of the solution. The remaining changes in the singular vectors are complex and less easy to interpret.

The significance S_j of the observables (cf. eq. [16]) is illustrated in Figure 4, for the reference case at distances of 1.3 and 100 pc. At 1.3 pc, it is evident that while most of the observables are very important in estimating the parameters, the colors $(b-y)_j$ and the small separations $(\delta\nu_0)_j$ are less important. At 100 pc this picture has changed, with the colors and small separations almost as important as the most significant observables, and the astrometric indices (except $P_{\rm orbit}$) playing lesser roles. This shift of emphasis occurs because the relative precision of the astrometry decreases as distance increases. The astrometric observations are thus less able to constrain the parameters at large distances, and other observables are used to supply (as best they can) the missing information.

The rms parameter errors for distances of 1.3 and 100 pc are shown in Figure 5. As explained above, these are defined to be the square root of the diagonal elements of the error covariance matrix (see eq. [14]), i.e., the errors in each parameter resulting from random errors in the observables, disregarding the (usually correlated) errors in other parameters. All of the errors increase as the distance increases, some dramatically. This is inevitable; information is lost by increasing the distance, and less information cannot improve the estimate of any parameter. The errors that increase the most are those corresponding to parameters that depend most strongly on the astrometric indices.

The loss of information resulting from ignoring the correlations between errors in parameter estimates is quite substantial. The product of twice the parameter errors plotted in Figure 5 equals the volume in parameter space of a box with edges parallel to the coordinate axes (i.e., the individual

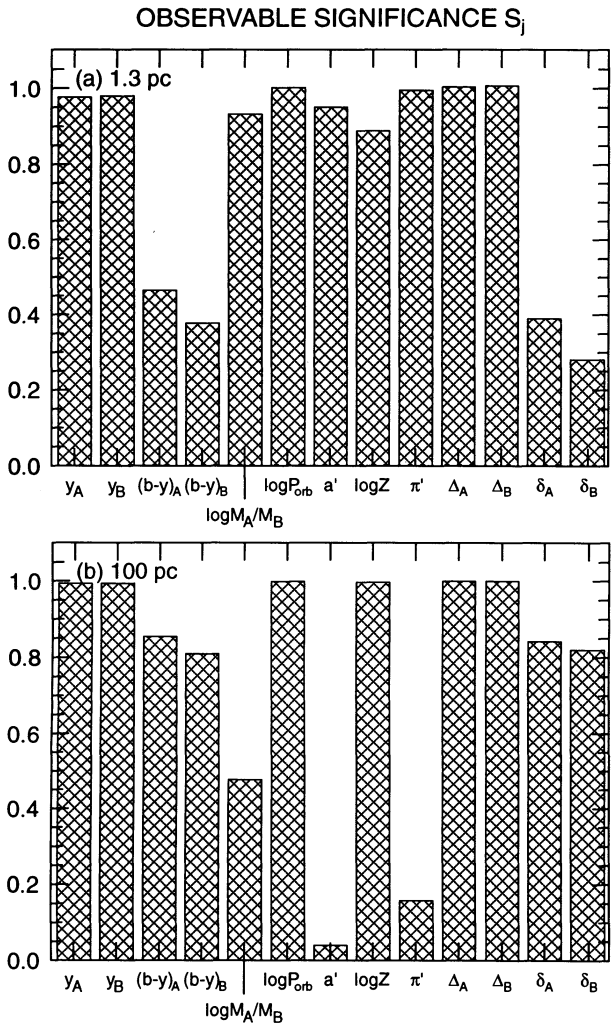

FIG. 4.—The significance (cf. eq. [16]) of observables in the reference case at distances of 1.3 pc (*a*) and 100 pc (*b*). Note the smaller role played by the astrometric indices at $D = 100$ pc, and the corresponding increase in the importance of the photometric colors and the small frequency separations $\delta\nu_0$.

parameters) that just contains the error ellipsoid. The product of twice the reciprocals of the singular values, in contrast, equals the volume of a box that also contains the error ellipsoid, but has its edges parallel to the ellipsoid's principal axes. For $D = 1.3$ pc, the ratio of these volumes is 1.3×10^7; for $D = 100$ pc it is about 10^{11}. To understand the origin of these huge ratios, imagine the wasted volume that would result if one were obliged to pack uncooked spaghetti strands, one to a box, in cubical containers just large enough for the strands to fit along the long diagonal. The very large ratio of largest to smallest singular values makes it unlikely that the error ellipsoid will pack neatly into a box aligned with the corrdinate axes. Thus, if one could properly account for the correlations between errors, the reduction in parameter space that need be considered would be roughly the same as if each of the parameter errors were reduced by an order of magnitude. This fact is a powerful incentive to frame theoretical questions, wherever possible, in terms of the combinations of parameters that are well constrained by observations. We recall that the principal axes of the error ellipsoid are given by the solution vectors $V^{(i)}$.

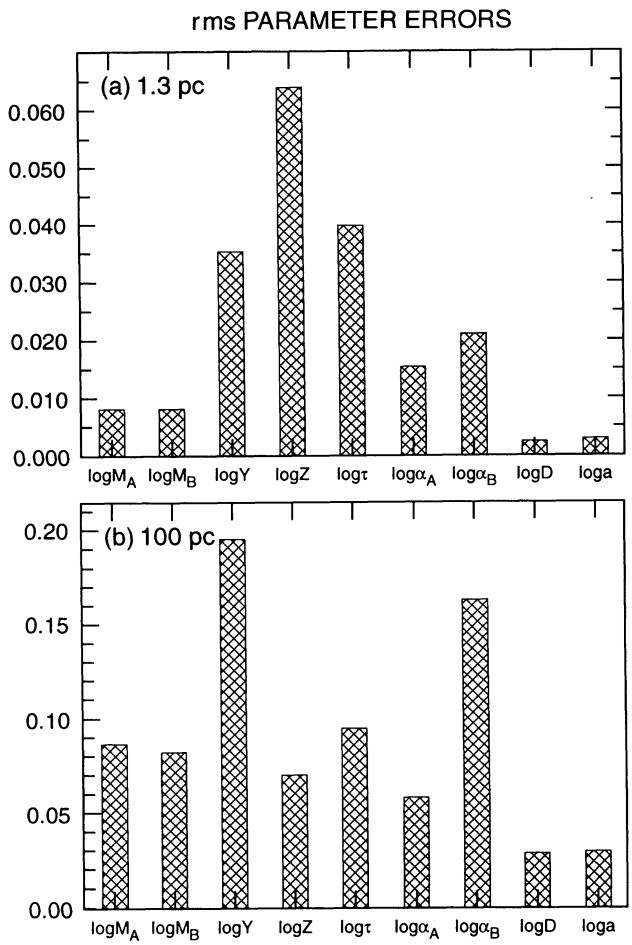

FIG. 5.—Expectation values of rms errors in the logarithms of the model parameters for the reference case, at distances of 1.3 pc (*a*) and 100 pc (*b*). Note the difference in scale between the two panels. The absence of reliable astrometric information at 100 pc leads to very large formal errors in the parameters.

Hence the favored combinations of parameters are determined by the $V^{(i)}$ corresponding to the largest singular values. From Figure 3*b* it follows that these combinations mainly involve the masses and composition of the two components; the resulting relations might be useful as constraints on stellar model calculations.

5.2. *Field Stars*

A reasonable model for an isolated field star requires six parameters (the five stellar structure parameters M, Y, Z, τ, α, and the distance D to the star). In the absence of oscillation data, however, the available observables number only four (m_y, $b-y$, Z_{obs}, and π'). In this case the solution is underconstrained; to get a solution it is necessary, as explained in § 4, to introduce explicit prejudices constraining the allowable ranges of at least two parameters. Figure 6 illustrates the parameter errors actually obtained using the prejudices listed in Table 2, for distances of 1.3, 10 and 100 pc. In this and subsequent plots, open bars signify the rms errors resulting from parameter estimates made without any oscillation data, single-hatched bars show the results if one parameterizes the frequencies using the large and small separations $\Delta\nu_0$ and $\delta\nu_0$, and cross-hatched bars show the errors if every second oscillation mode in the range $17 \leq n + l/2 \leq 29$ is present, correctly identified, and has an individually known frequency. Since

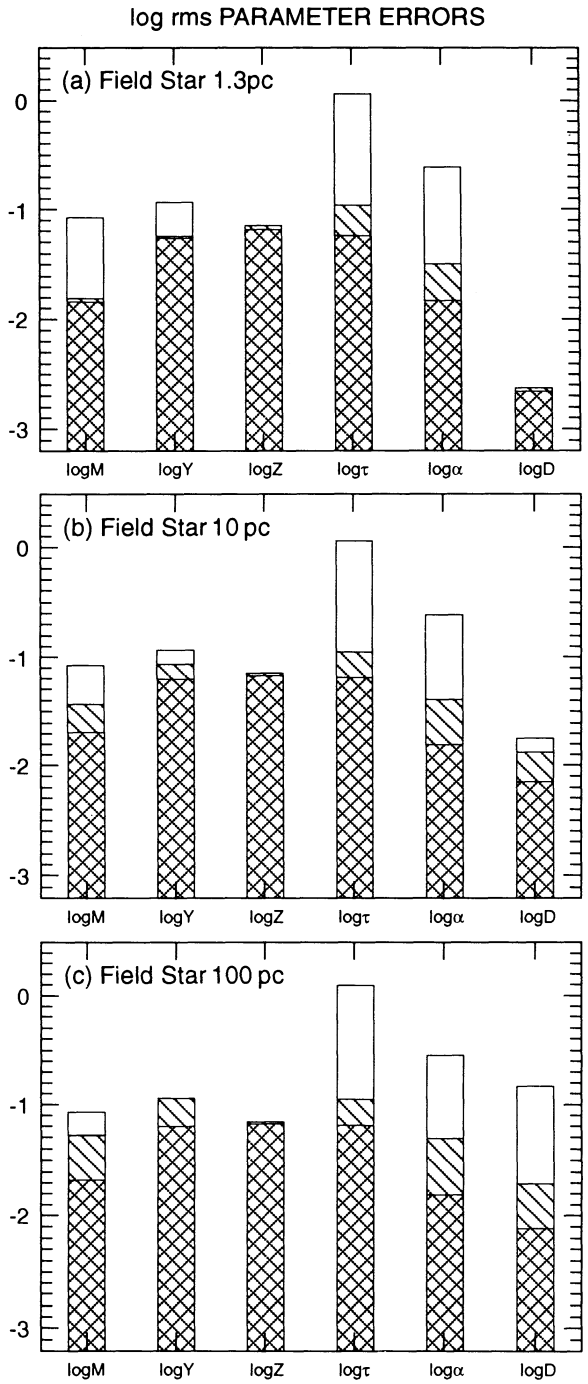

FIG. 6.—Formal parameter estimation errors for a field star at distances of 1.3, 10, and 100 pc (panels *a*, *b*, *c*, respectively.) In this and the following bar plots, open bars indicate the errors that result if no oscillations data are available. Single-hatched bars show the errors if the two frequency separations are included among the observables, and cross-hatched bars show the errors if individual mode frequencies are available. Note that the quantities plotted are the $\log_{10}$ of the errors; since the parameters are themselves logarithms of the relevant physical quantities, these plots approach the ideal of graphical astronomy: to display the log of the log of some quantity along each plot axis.

each of these steps involves additional information, the errors are always largest for the open bars, and smallest for the cross-hatched bars.

Figure 6*a* shows that, even at 1.3 pc, the age and helium abundance are constrained entirely by the imposed prejudices.

Adding frequency separation data leaves the errors in metallicity and distance essentially unchanged, but makes substantial improvements (about a factor of 10) in the precision of estimates of age and mixing length, a somewhat smaller improvement in the mass estimate, and a relatively modest change (not quite a factor of 2) in the precision of the helium-abundance estimate. Providing complete frequency information, in this case, has relatively little effect: one obtains only small decreases in the errors in τ and α.

Panels *b* and *c* of Figure 6 illustrate the rms parameter errors at distances of 10 and 100 pc. Since increasing distance degrades one's information about the star only by decreasing the relative precision of the parallax measurement, the only major change in the errors is that the distance estimate gets worse with increasing distance. A smaller effect is that the difference between having only mode separations and having mode frequencies increases with increasing distance; evidently the extra information in the mode frequencies becomes more important as the quality of the astrometry declines.

While the improvements in errors due to the addition of oscillation information appear impressive, one should recall that the actual error levels attained for field stars are likely to be useful only in certain circumstances. For the full-frequency information case in Figure 6*a*, the remaining errors in mass and in mixing length are about 3%; in age, 12%; in helium abundance, 12% (i.e., $Y = 0.28 \pm 0.035$). Except for the error in Y (which is uninterestingly large for almost any application), errors at the level just described would suffice for an improved understanding of local stellar properties, if they could be obtained for a substantial number of stars. Errors of this size are likely to prohibit tests of the basic physics underlying stellar structure theory, however. To perform tests of this sort, more information will likely be necessary.

5.3. *The Reference Case (Revisited)*

As indicated in § 1, what is desired for testing of underlying physical ideas may be available in the case of visual binary systems. We thus return to the "reference" case described in § 5.1. The rms parameter errors for this case, with three different levels of oscillation data, are illustrated in Figure 7 for distances of 1.3 pc, 10 pc, and 100 pc. (Note that the results including frequency separations at 1.3 and 100 p.c, shown as single-hatched bars, were already presented in Fig. 5.) Figure 7*a* shows the rms errors for the standard case at $D = 1.3$ pc. In this case, the addition of oscillation data has little effect except on the estimates of the mixing lengths and (to a lesser extent) the age. The use of complete mode frequency information (as opposed to separations alone) makes little difference. In this instance, the photometric and astrometric observations are evidently so accurate that they suffice to yield a good definition of the stellar system; the addition of oscillation frequencies is relatively unimportant. If one's aim is to estimate stellar parameters this is perhaps disappointing, but from the viewpoint of testing stellar evolution theory, it is precisely what one wishes to see. Since the new observations are giving information that is largely redundant with existing data, one can meaningfully search for inconsistencies between the observations that point to inadequacies in the model.

Figure 7*b* shows the case in which $D = 10$ pc. This case is quite different from the previous one, in that estimates for all of the parameters except Z are substantially improved by the addition of frequency-separation information. Of the remaining parameters, all but the age and mixing lengths see dramatic

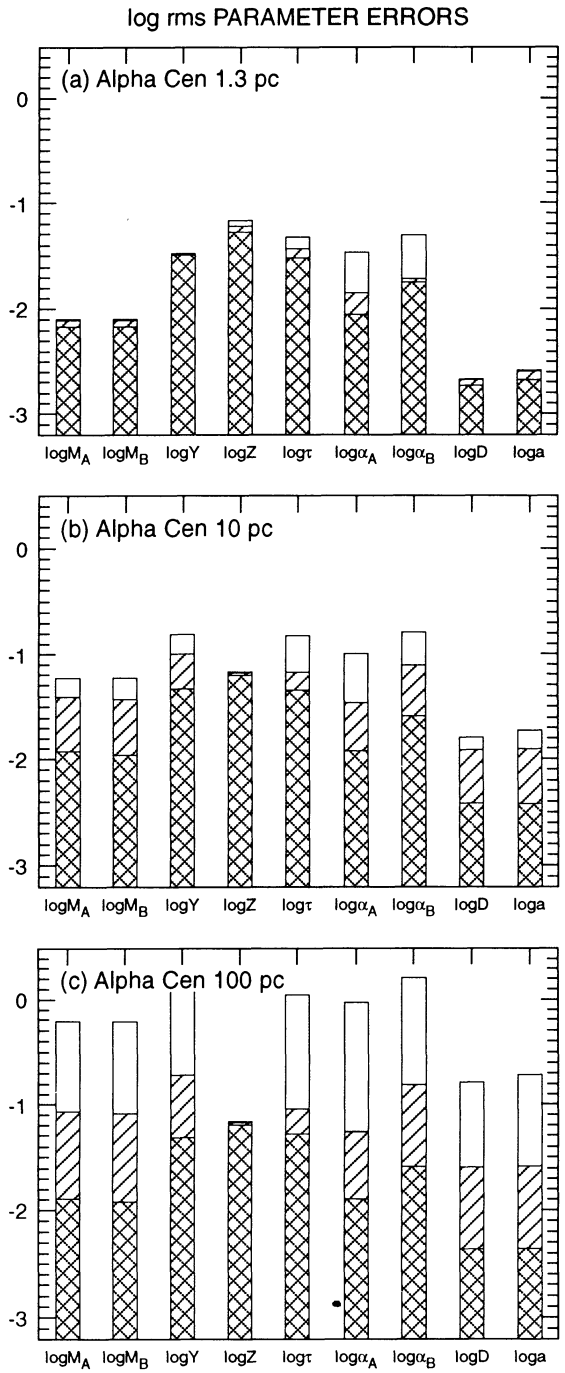

FIG. 7.—Same as Fig. 6, but for the α Cen reference system

further improvement when full mode frequency information is included. This behavior illustrates the importance of the very precise astrometric data that are available in the $D = 1.3$ pc case. As the distance to the system increases, the relative precision of the astrometric measurements gets rapidly worse, increasing the impact of new information.

Figure 7*c*, for the case $D = 100$ pc, shows the natural extension of the trend begun in Figure 4*b*. Here the distance is sufficiently large that astrometric data are essentially worthless, and the photometric data alone are insufficient to con-

strain the stellar models. (Note that without oscillation data, the formal rms errors are for all parameters larger than the prejudices given in Table 2. This occurs because the prejudices are not included as constraints in the analysis of the binary star cases.) In this situation, the addition of pulsation information makes a tremendous difference, especially if one has mode frequencies and not just separations. The heavy-element abundance Z is a notable exception to this rule; although the oscillation frequencies depend on Z, this dependence evidently cannot be separated from the dependence on other parameters, and hence does not serve as a useful constraint. It is also worth noting that the estimates for Y, for the mixing lengths, and for the masses, though much improved by oscillation data, are still sufficiently uncertain as to be relatively uninteresting. The principal utility of oscillation data in this instance is to provide a length scale for the system, which when combined with the photometry leads to an accurate distance estimate. This may prove to be an important feature if stars with Sun-like pulsations can be identified in open clusters, where the distance uncertainty is an impediment to isochrone fitting.

5.4. *Variations on the Reference Case*

While the conclusions in the reference case are interesting in themselves, it is unlikely that they will apply unaltered to any real binaries with the exception of α Cen itself. It is therefore important to understand to what extent the conclusions depend on attributes of the reference case that may not be common to other systems. In this section we shall consider several such modifications to the reference case.

While modes with angular degree $0 \leq l \leq 3$ should be observable in Doppler-shift observations, photometric observations will be sensitive only to the smaller range $0 \leq l \leq 2$ (e.g., Dziembowski 1977). Figure 8 shows the effect of including in the analysis only modes within this smaller range of l, for the case in which $D = 1.3$ pc. Comparison with Figure 7*a* shows that the differences in error bars are negligible in this case. As might be expected from the previous discussion, the changes are slightly larger for greater distances, but even at $D = 100$ pc they are not very important.

Another likely circumstance is that one may observe a system in which only one of the stars is seen to pulsate. Figure 9*a* shows the rms errors in the case that oscillation frequencies are available only for the brighter of the two components, and for $D = 1.3$ pc. The most important difference between this and the standard case is that with a single set of pulsation frequencies, the mixing length of the fainter component becomes less well determined. As the distance to the system increases (Fig. 9*b*), even this difference disappears. As noted above, at large distances the most important information contained in the oscillation frequencies seems to be an estimate of the dis-

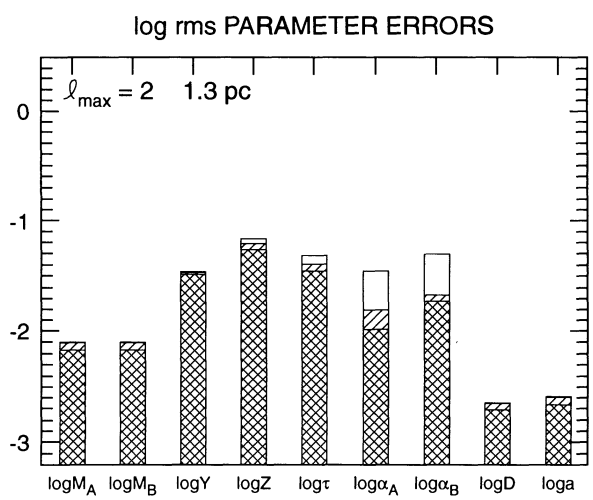

FIG. 8.—Same as Fig. 7, but for the case in which the range of angular degree observed is $0 \leq l \leq 2$. Only results for $D = 1.3$ pc are shown, since for the larger distances the errors are virtually identical to those in Fig. 7.

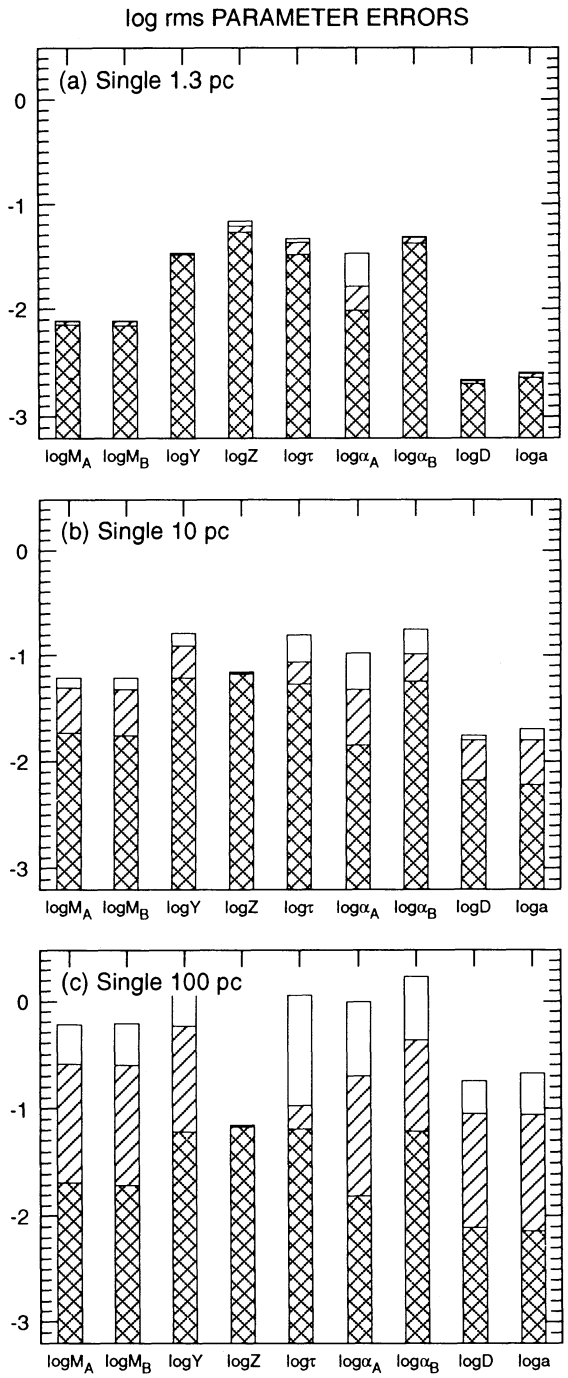

FIG. 9.—Same as Fig. 7, but for the case in which only the brighter component (A) is assumed to have observable oscillations.

tance itself, and for this purpose one set of frequencies is not much worse than two.

Next (Fig. 10) we imagine that we are willing to model the system using only a single value of the mixing length, which is presumed to apply to both stellar components. The main difference between this and the standard case is that the composition parameters (particularly Y) become better defined. Evidently the structural changes resulting from changes in the mixing length can be well approximated (at least insofar as the oscillations can tell) by changes due to composition; constraining the mixing length then permits more of the oscillation frequency information to be used to determine Y and Z.

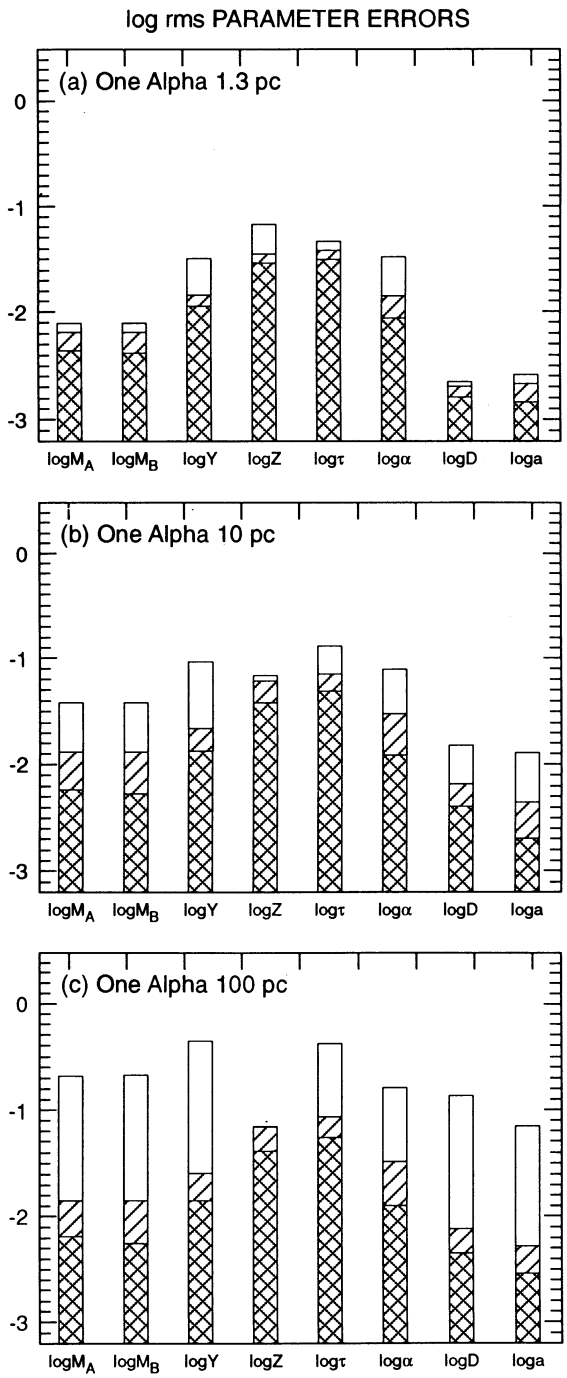

FIG. 10.—Same as Fig. 7, but for the case in which a single mixing length is assumed to describe both stars.

5.5. *Improvements in Other Observations*

Since it will clearly be difficult to obtain good pulsation information about Sun-like stars, one may reasonably ask whether a similar or better improvement in our ability to estimate parameters would result from improvements to the photometry or astrometry. A natural expectation is that pulsation frequencies contain different kinds of information than are found in the other sorts of observations, so that it is unlikely that oscillation data can be replaced with more precise data of other sorts. Also, it is clear that reducing errors in existing observations will not lead to overconstrained systems, thus allowing tests of physical assumptions. It is at least conceivable, however, that oscillation and other kinds of observations are largely redundant. To examine this possibility, we have performed tests in which the precision of the photometry or astrometry has been significantly improved.

Figure 11 shows the situation when the photometric errors (both magnitudes and colors) are reduced from their standard values by a factor of 3. There are no fundamental reasons why errors of this size (1.6 mmag in both magnitude and color) cannot be achieved from the ground, but doing so would certainly represent a noticeable improvement on current practice. Comparison with Figure 7 shows that at 1.3 pc and in the absence of oscillation data, the only significant changes (about a factor of 2) accompanying these reduced photometric errors are in the errors associated with the mixing lengths. Even for these two parameters, however, the improvements due to photometry are not as large as those due to the addition of frequency difference information in the reference case. Adding oscillation data to improved photometry again makes the largest change in the estimates of the mixing lengths, and once again the change is not very large. At larger distances (Figs. 11*b* and 11*c*), the improvements resulting from better photometry alone vanish altogether. Better photometry combined with oscillations continues to yield some gains in precision, but once again the effects are rather small.

In Figure 12, we have assumed that the errors in parallax, semimajor axis, and mass ratio have all improved over the reference case by a factor of 3. The error in orbital period was not changed, since this error depends so heavily on the temporal baseline of existing observations. Better technology is therefore unlikely to make rapid or substantial changes in the precision with which $P_{\rm orbit}$ is known for any star. This case at 1.3 pc distance is quite different from the photometric one, in that better astrometry leads to roughly proportional improvement in the errors for several parameters: the stellar masses, the distance, and the semimajor axis. These parameters are the ones that would naturally be thought of as depending on the astrometric indices. For all these parameters, the improvement is greater than that which results from adding oscillation data (even with full frequency information) in the reference case. The reduction in astrometric errors makes the introduction of oscillation data more helpful for some parameters and less so for others, but in no case is the change very important. At distances greater than 1.3 pc, the impact of better astrometry is smaller, as one would expect.

5.6. *Testing Physical Assumptions*

As already stated, one of the principal motivations for pursuing the study of pulsations in other stars is to test assump-

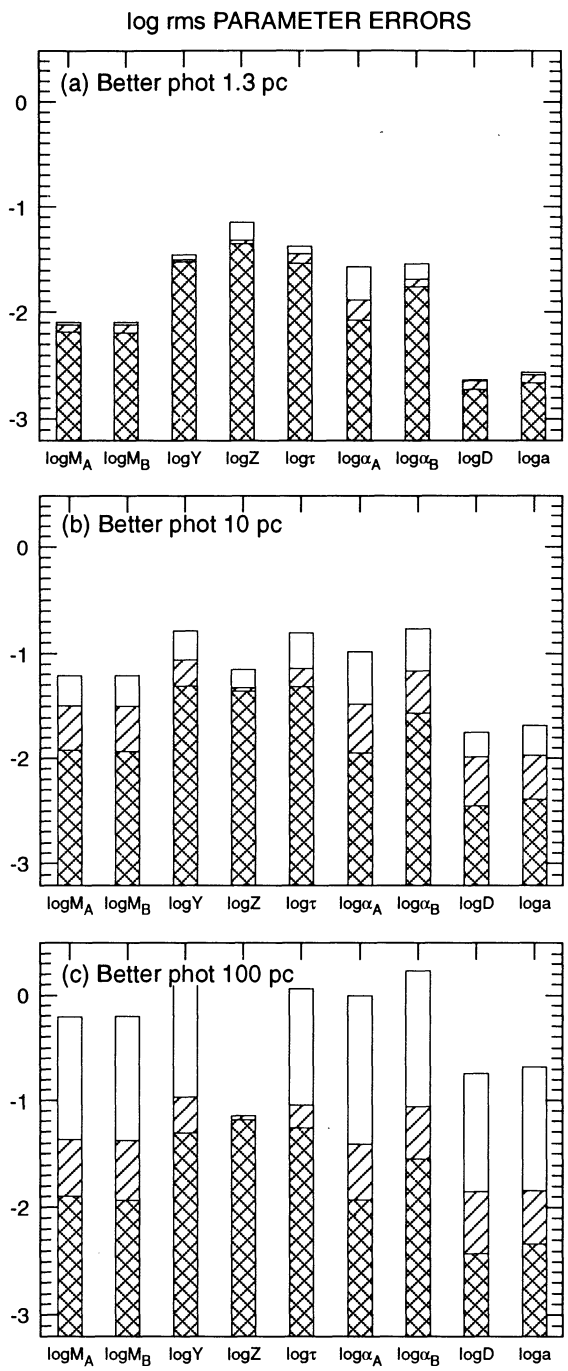

FIG. 11.—Same as Fig. 7, but for the case in which the precision of the photometric indices is assumed to have improved by a factor of 3.

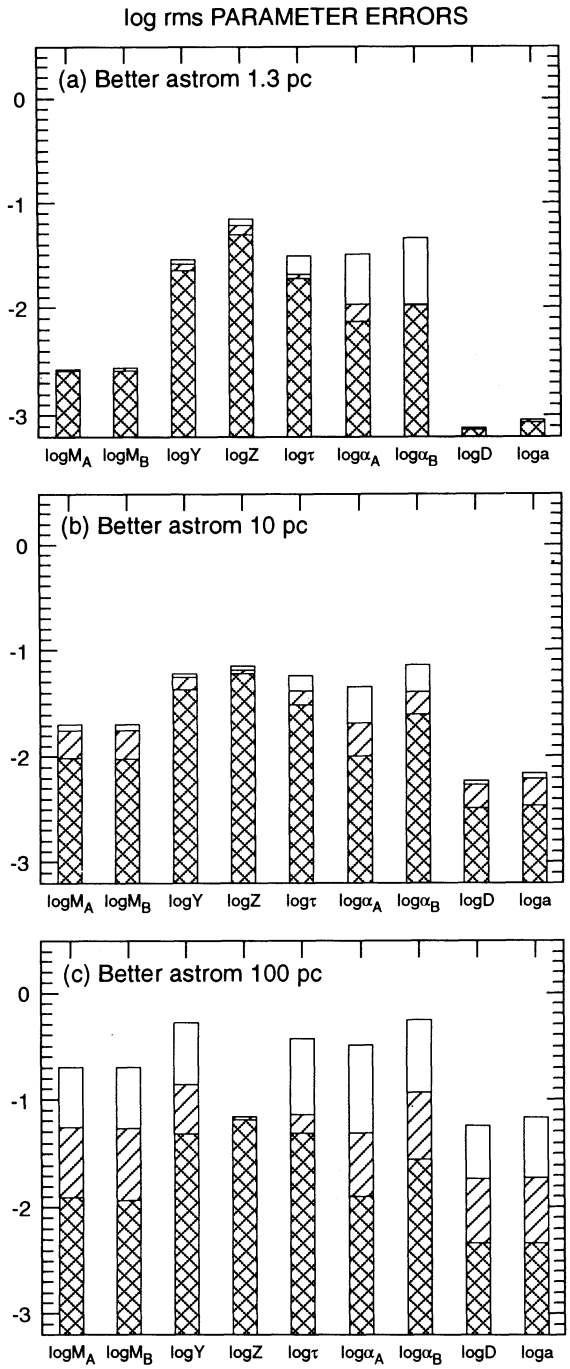

FIG. 12.—Same as Fig. 7, but for the case in which the astrometric indices (except P_{orbit}) are assumed to have improved by a factor of 3.

tions concerning the physics underlying stellar structure theory. To investigate the practicality of this idea, we constructed four models of the α Cen system that generally use the same parameter values as the reference model but incorporate plausible changes in the physical assumptions. These are listed in Table 4 as cases II–V, case I being the reference model. The first model used the so-called CEFF equation of state (Christensen-Dalsgaard & Däppen 1992), where Coulomb effects have been added to the basic Eggleton et al. (1973) formalism. In the remaining models, the opacities were obtained from the Livermore OPAL tables (Rogers & Iglesias 1992; Iglesias, Rogers, & Wilson 1992), matched smoothly, near $T = 10^4$ K, to the low-T opacities of Kurucz (1991). Case III was otherwise identical to the reference case. In particular, the same value of the mixing-length parameter α was used; since the OPAL opacities are substantially smaller than the LAOL opacities in the atmosphere, this induces a significant increase in the depth d_b of the convection zone. For the purpose of testing the effects of diffusion and gravitational settling which depend sensitively on d_b, case IV was computed,

with α reset to the value 1.8371 required to calibrate a solar model with the OPAL opacities. Finally, the fourth model used the OPAL opacities and this value of α, but in addition allowed for gravitational settling of helium from the stellar convection zones into the radiative interiors, according to the procedures of Michaud & Proffitt (1993) and Christensen-Dalsgaard, Proffitt, & Thompson (1993).

When testing the effects of these modifications on the frequencies, we considered pairs of models where only one aspect had been changed; we have not considered combinations of the effects. Figure 13 shows the relative frequency differences induced by changing the opacity or equation of state, or by introducing gravitational settling, after correction for the change in radius. As mentioned above, the opacity change causes substantial changes in the atmospheric structure of the model, which are reflected in a component of the frequency differences which vary little with degree and slowly with frequency. However, the l-dependence of $\delta\nu$ in this case indicates that there are also differences in the core of the model. In contrast, the differences resulting from a change in the equation of state or from helium settling are dominated by an oscillatory behavior coming from changes in the second helium ionization zone; this results directly from the change of the equation of state in the former case, and from the change in envelope abundance due to settling in the latter.

The procedure we used to test the influence of errors in the physics on the parameter determination was to calculate observables based on the new physical assumptions, and then to use the SVD procedure to estimate parameter changes that would best match the new observables to models with the reference physics. In general, such parameter changes in an incorrect model cannot exactly reproduce all of the changes in the observables, so some residual errors remain. The central question is whether the residual errors are observationally significant. If the residuals are all small compared to the observational errors, it is not possible to distinguish parameter changes from changes in physical assumptions. In general, we find that stars obeying different physics succeed remarkably well in masquerading as stars that merely have different parameters. There are distinctions, however, and in many cases those distinctions appear to be large enough to be detectable.

We first consider the effect of changing the opacity law (case III–case I), for a system at 1.3 pc. Modifications to the observables are large in this case: roughly 6 σ in the magnitudes, 11 σ in the colors, and typically 150 σ in the frequencies of individual modes, leading to some 200 σ in the large separation $\Delta\nu_0$. The small frequency separation does not change perceptibly, and of course the astrometric indices remain unchanged by variations in the stellar model physics. For the most part, however, the very large changes in mode frequencies arise from changes in the stellar radius. These are easily simulated within the framework of the reference model mostly by decreasing the metallicity Z (by a factor of 1.7) and increasing the mixing lengths (by factors of 1.3–1.5).

Figure 14 shows the residuals in the observables that remain after subtracting the effects of the parameter changes. Several

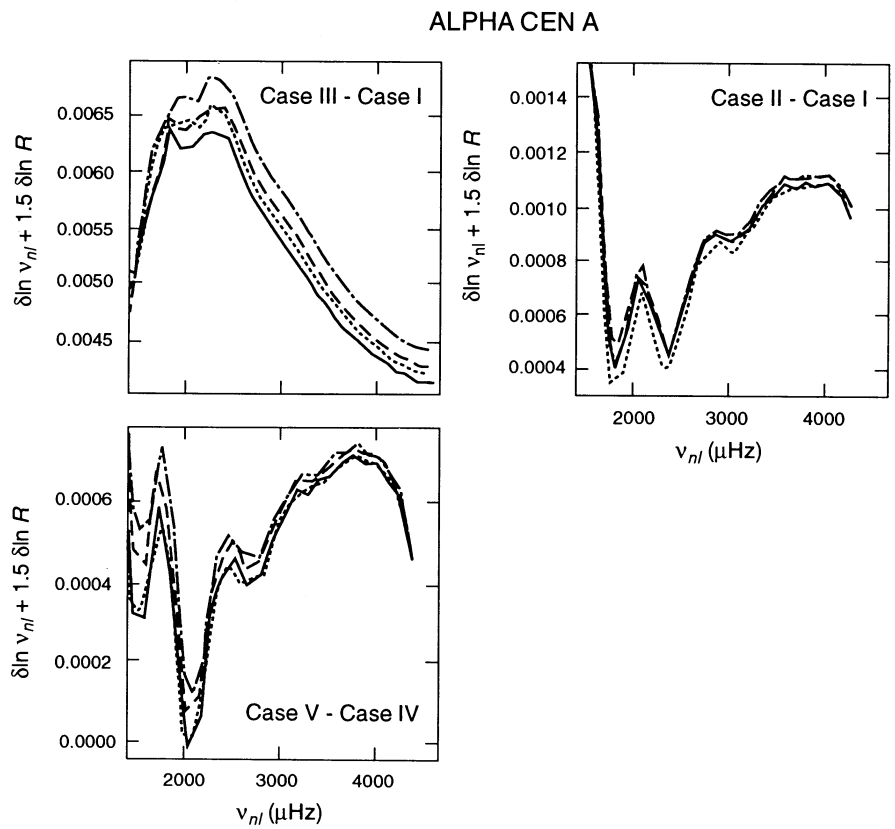

FIG. 13.—Changes in $\ln\nu$ resulting from changes in the assumed physics, after correction for the change in mean density according to eq. (1). Each line corresponds to a different value of the degree l, the same line styles being used as in Fig. 2. The cases are labeled as in Table 4. Panel (*a*) shows the result of changing the opacity, panel (*b*) the equation of state, and panel (*c*) the effect of including helium settling. Note that, as in Fig. 2, the largest changes are functions of frequency alone, although opacity changes do result in frequency changes with some l dependence.

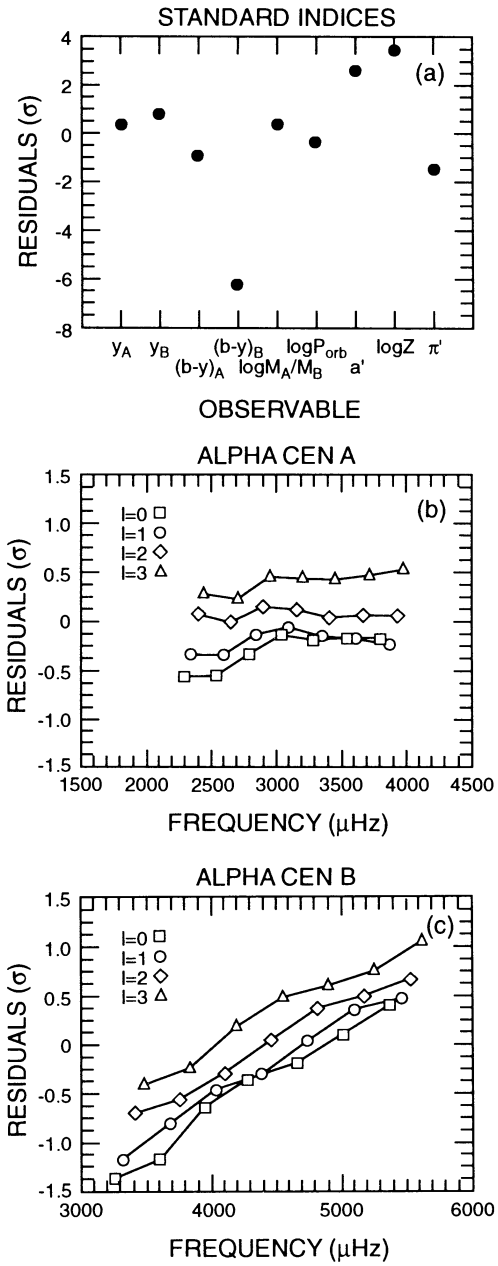

FIG. 14.—Residuals in the observables resulting from changing from LAOL to OPAL opacities (Case III–Case I), after subtracting that portion of the observable changes that can be generated by changing the model parameters. (*a*) Changes in the photometric, astrometric, and spectroscopic indices. (*b*) *p*-mode frequency shifts as a function of frequency for α Cen A. Different symbols indicate different values of *l*, as shown in the figure. (*c*) Frequency shifts for α Cen B. All residuals are plotted in units of the standard error of the corresponding observable.

of the observables not related to oscillations (notably the color of component *B*, the spectroscopic metallicity, and the apparent semimajor axis) show very significant (up to 6 σ) discrepancies in this case. The residuals in the oscillation frequencies are not as large, scarcely exceeding 1 σ. The frequency residuals, especially those for the B component, show a distinctive variation with *l* and frequency, however; if a reasonable fraction of the modes shown in Figure 14 were actually detected, this behavior would be readily apparent even though the errors for single modes are about the same size as the residuals. In this case, therefore, the reference model clearly fails to reproduce the observations, giving strong evidence for incorrect physical assumptions. We note, however, that the dominant frequency-dependent trend in the residuals would be difficult to distinguish from frequency errors caused by an inadequate treatment of the oscillations in the near-surface layers (including, e.g., the use of the adiabatic approximation).

For the model with a modified equation of state (case II–case I) seen at 1.3 pc, the situation is somewhat different than for a modified opacity. The changes in the observables in this case are mostly smaller than in the previous one (15 σ for the magnitudes, 2–4 σ for the colors, and less than about 50 σ for the mode frequencies.) The model parameter adjustments required by the fit to the new observations are, however, smaller yet: the largest changes are decreases of roughly 7% in Z and 4% in τ. The observational residuals following this parameter adjustment are shown in Figure 15. Again, by far the greatest part of the mode frequency variation is well reproduced by parameter changes within the framework of the reference model; the part of the variation that cannot be explained by simple parameter changes is at most only about 0.5 σ. The frequency variation of the residuals is again quite systematic, with an oscillatory signature that is probably related to the changes in the second helium ionization zone; the small amplitude would make its unambiguous identification problematic, however. The parameter adjustments do less well at reproducing changes in the other observables. The worst match (3.5 σ discrepancy) is with the color of the B component, while the parallax shows a discrepancy of about 1 σ. Other astrometric and photometric indices are in error by typically 0.4 σ. In this case, it appears that *p*-mode observations would constrain the model so as to cause suspiciously bad fits with other observations. At the assumed levels of observational error, however, it is unlikely that one could unambiguously determine the reason for the bad fits.

Finally, Figure 16 illustrates the residuals for the case in which diffusion of helium out of the convection zone has been allowed (case V–case IV). The observable changes resulting from this modification to the physics are even smaller than in the previous cases: 1–2 σ for the photometric indices and less than about 40 σ for the mode frequencies. The model parameter adjustments required to match the new observables consist mainly of changes in the mixing lengths (decreases of 6% and 10% for components A and B, respectively), and a 10% increase in the model metallicity. These changes are qualitatively similar to those inferred above when changing the opacity, but are opposite in sign and substantially smaller in magnitude. The residuals after adjusting the model parameters are evidently quite small. The observables with the largest residuals are the colors and Z, but none of these is larger than 0.6 σ. The frequency residuals for the A component show an oscillatory dependence on frequency, reflecting the change in the envelope helium abundance, but the magnitude is small; for the B component, where the deeper convection zone decreases the effect of settling, this effect is barely visible. Evidently the effect of helium diffusion (at least in these stars of approximately solar mass) would not be possible to discern with observations of the quality that we have considered here.

6. DISCUSSION

One of our aims in undertaking this study was to help determine whether the benefits of oscillation data are sufficient to

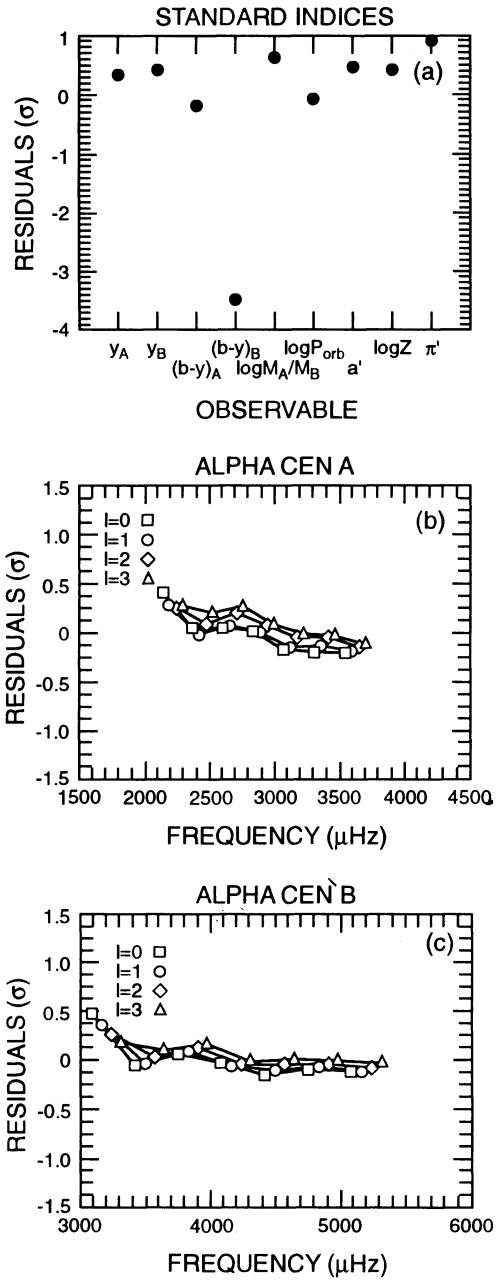

FIG. 15.—Same as Fig. 14, except showing the observable residuals caused by changing from the EFF to the CEFF equation of state (Case II–Case I).

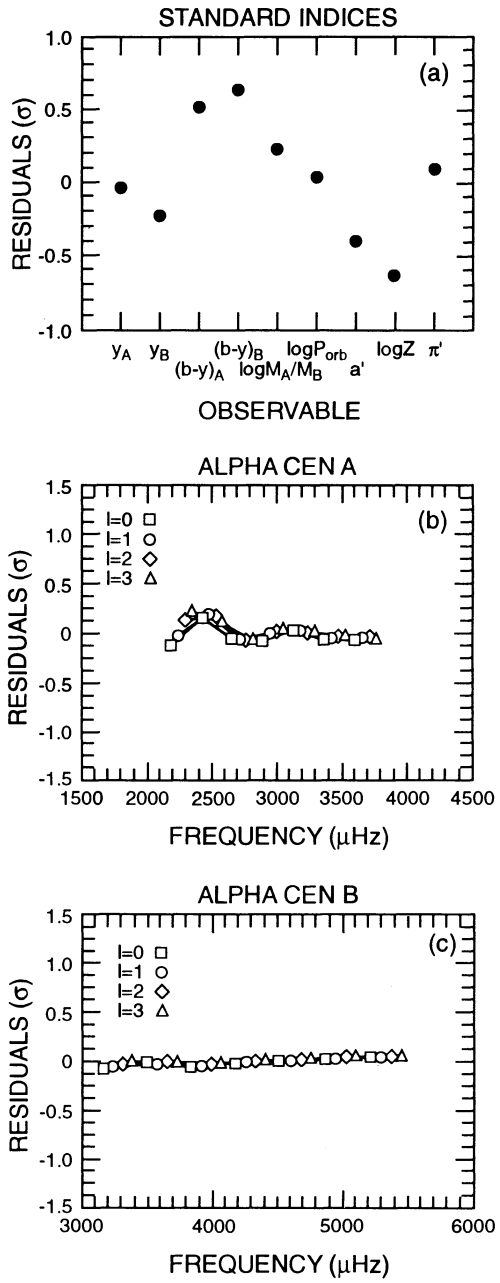

FIG. 16.—Same as Fig. 14, except showing the observable residuals caused by inclusion of gravitational settling of helium from the stellar convection zones (Case V–Case IV).

justify the cost and effort of obtaining them. The foregoing results suggest that the observational effort is indeed worthwhile. At the same time, this study illustrates the vital importance of combining oscillation data with high-quality information from other sources, and of seeking out stellar systems for which the observations can be used to best advantage. Assuming that these things are done, it appears that stellar oscillation frequency measurements can make a substantial contribution to our knowledge of the structural parameters of stars. Though the precision of estimates of mass, age, and mixing length can be significantly improved, unambiguous information about the composition will be harder to obtain. Moreover, in favorable circumstances the oscillation frequencies will allow direct investigation of at least some aspects of the physics that underlies the theory of stellar structure. Questions about the opacity of stellar material appear particularly approachable in this way, and those relating to the equation of state may be within reach. The role played by gravitational settling of helium, however, appears to be difficult or impossible to separate from other effects, given observations of the precision that we assume.

The current understanding of the excitation of solar-like oscillations is not adequate to predict the probability of finding binary systems where both components display detectable

oscillations. Furthermore, given the constraints involved in detecting the expected very small signal, it is likely that in many cases it will not be possible observationally to separate the two components; evidently the likelihood of this situation increases with the distance to the system. In such cases, it is probable that the observed oscillations will be entirely dominated by those of the brighter component of the system, the oscillations of the fainter component, even if present, being undetectable. The results obtained in § 5.4 indicate that the lack of oscillation data for one component will not seriously compromise the determination of the parameters of the system.

Our results are complementary to recent work on inversions of simulated stellar oscillation frequencies. Gough & Kosovichev (1993a, b) carried out inverse analyses for the relative differences in density and $u = p/\rho$, p being pressure, as a function of relative position in the star. They found that it was possible to obtain localized measures of these quantities in the core of the star, provided that modes of order as low as 5 were included. Kosovichev (1993) performed the inversion in terms of the convective stability measure A^* and the helium abundance, using modes in a frequency interval roughly corresponding to the one considered here. From artificial data he was able to determine the helium abundance and the location of the base of the convective envelope with considerable precision, although application to the IPHIR data on solar oscillations (Toutain & Fröhlich 1992) was somewhat less successful. There are two significant differences between these efforts and ours. First, they are concerned with measuring the depth dependence of quantities that can be estimated without the necessity of a full and consistent model of the star. Second, the precision assumed for oscillation frequency measurements is a factor of 20 better than the value which we use. Availability of mode frequencies with this assumed precision (0.1 μHz) would significantly strengthen many of our conclusions.

The importance of combining different kinds of information (oscillation frequencies, photometry, astrometry, spectroscopy) cannot be overemphasized. These different indices respond to various aspects of stellar structure in different ways; only by combining them can anything like a comprehensive picture of the star be obtained. In this connection, we note that there are several kinds of observations that might have been considered here, but were not. Photometric indices other than m_y and $b - y$ were mentioned briefly in § 4.1, but we have not pursued this further. More detailed spectroscopic information (for instance, estimates of $\log g$, $T_{\rm eff}$, stellar magnetic activity, or of details of the heavy-element abundances) may be even more useful. Further information, particularly on stellar radii, can be obtained in the case of detached double-line eclipsing binary systems, which even in the absence of oscillation data provide stringent constraints on stellar evolution theory (e.g., Andersen 1991); in such cases it is unlikely that more than one oscillation spectrum can be clearly identified, however. Oscillation measurements may also provide a number of observables besides mode frequencies. These include the rotational splittings of modes with $l > 0$, and the lifetimes and mean amplitudes of all the modes. Frequency splittings provide information about the depth dependence of the stellar rotation (e.g., Gough 1981). Combined with a surface rotation rate derived from precision photometry or from spectroscopy, such information would help answer questions about the flow of angular momentum within the stars (e.g., Stauffer 1991; Charbonneau 1992). The amplitude and lifetime information is less useful at present, because of the relatively undeveloped state of theories describing these phenomena. It is reasonable to suppose, however, that future advances along these lines should yield fairly detailed information about the dynamics of the upper parts of stellar convection zones and about the conditions (such as surface gravity) that influence them. Analysis of star clusters should provide information of yet a different sort, since they provide the opportunity to examine many stars of different mass but with similar composition and age. Gough & Novotny (1993) have begun to assess the potential of oscillation measurements within star clusters; we are presently engaged in a companion study to the current one, applying the SVD approach to existing and anticipated observations of clusters of stars.

Finally, we repeat that the sensitivities of derived stellar parameters to errors in the observations depend on the system under study and on the circumstances of observation in complicated ways. Simple approximations to the dependences are often misleading, so that some suitably general form of analysis (such as the SVD formalism) is required. In the current case the SVD approach does not yield simple physically motivated relations between the observables and the parameters. This is not a flaw in the technique, it is simply a feature of the transformation that connects parameters and observables. In its favor, the SVD formalism allows a precise understanding of the transformation under consideration, so that interpretational problems may be identified and opportunities assessed. We recommend its use in problems of parameter estimation that involve numerous parameters or observables with disparate properties.

We thank F. J. Rogers, C. A. Iglesias, and R. L. Kurucz for providing us with opacity data, and W. Däppen and G. Houdek for help with implementing these opacities in our calculations. The computations reported here were supported in part by the Danish Natural Science Research Council.

REFERENCES

Anders, E., & Grevesse, N. 1989, Geochim. Cosmochim. Acta, 53, 197
Andersen, J. 1991, Astron. Astrophys. Rev. 3, 91
Brown, T. M., & Gilliland, R. L. 1990, ApJ, 350, 839
Brown, T. M., Gilliland, R. L., Noyes, R. W., & Ramsey, L. W. 1991, ApJ, 368, 599
Charbonneau, P. 1992, in Seventh Cambridge Workshop on Cool Stars, Stellar Systems and the Sun, ed. M. S. Giampapa & J. A. Bookbinder (ASP Conf. Ser., 26), 416
Christensen-Dalsgaard, J. 1982, MNRAS, 199, 735
———. 1984, Space Research Prospects in Stellar Activity and Variability, ed. F. Praderie (Paris: Paris Observatory Press), 11
———. 1988, in IAU Symp. 123, Advances in Helio- and Asteroseismology, ed. J. Christensen-Dalsgaard & S. Frandsen (Dordrecht: Reidel), 295
Christensen-Dalsgaard, J., & Berthomieu, G. 1991, in Solar Interior and Atmosphere, ed. A. N. Cox, W. C. Livingston, & M. Matthews (Tucson: Univ. Arizona Press), 401
Christensen-Dalsgaard, J., & Däppen, W. 1992, Astron. Astrophys. Rev., 4, 267
Christensen-Dalsgaard, J., Proffitt, C. R., & Thompson, M. J. 1993, ApJ, 403, L75
Courtaud, D., Damamme, G., Genot, E., Vuillemin, M., & Turck-Chièze, S. 1990, Sol. Phys., 128, 49
Demarque, P., Guenther, D. B., & van Altena, W. F. 1986, ApJ, 300, 773
Dziembowski, W. A. 1977, Acta Astron., 27, 203
Edmonds, P., Cram, L., Demarque, P., Guenther, D. B., & Pinsonneault, M. H. 1992, ApJ, 394, 313
Edvardsson, B., Andersen, J., Gustafsson, B., Lambert, D. L., Nissen, P. E., & Tomkin, J. 1993, A&A, in press
Eggleton, P. P., Faulkner, J., & Flannery, B. P. 1973, A&A, 23, 325
Flannery, B. P., & Ayres, T. R. 1978, ApJ, 221, 175
Furenlid, I., & Meylan, T. 1990, ApJ, 350, 827
Gelly, B., Grec, G., & Fossat, E. 1986, A&A, 164, 383
Gilliland, R. L., et al. 1993, AJ., in press

Gómez, A. E. 1993, in IAU Colloq. 137, Inside the Stars, ed. W. Weiss (ASP Conf. Ser., 40), 324
Gough, D. O. 1981, MNRAS, 196, 731
———. 1987, Nature, 326, 257
———. 1990a, in Astrophysics. Recent Progress and Future Possibilities (Mat.-fys. Meddel. Kgl. Danske Vidensk, Selsk), 42, no. 4, 13
———. 1990b, Progress of Seismology of the Sun and Stars, ed. Y. Osaki & H. Shibahashi (Lecture Notes in Physics 367), 283
Gough, D. O., & Kosovichev, A. G. 1993a, in IAU Colloq. 137, Inside the Stars, ed. W. W. Weiss (ASP Conf. Ser., 40), 541
———. 1993b, in Proc. GONG 1992; Seismic Investigation of the Sun and Stars, ed. T. M. Brown (ASP. Conf. Ser., 42), 351
Gough, D. O., & Novotny, E. 1993, in Proc. GONG 1992: Seismic Investigation of the Sun and Stars, ed. T. M. Brown (ASP Conf. Ser., 42), 355
Huebner, W. F., Merts, A. L., Magee, N. H., & Argo, M. F. 1977, Astrophysical Opacity Library, Los Alamos Scientific Laboratory Report LA-6760-M
Iglesias, C. A., Rogers, F. J., & Wilson, B. G. 1992, ApJ, 397, 717
Innes, J. L., Isaak, G. R., Speake, C. C., Brazier, R. I., & Williams, H. K. 1991, MNRAS, 249, 643
Kamper, K. W., & Wesselink, A. J. 1978, AJ, 83, 1653
Kosovichev, A. G. 1993, MNRAS, in press
Kurucz, R. L. 1991, in Stellar Atmospheres: Beyond Classical Models, ed. L. Crivellari, I. Hubeny, & D. G. Hummer (Dordrecht: Kluwer), 441
Michaud, G., & Proffitt, C. R. 1993, in IAU Colloq. 137, Inside the Stars, ed. W. W. Weiss (ASP. Conf. Ser., 40), 246
Parker, P. D. 1986, Physics of the Sun, Vol. 1, ed. P. A. Sturrock, T. E. Holzer, D. Mihalas, & R. K. Ulrich (Dordrecht: Reidel), 15
Pottasch, E. M., Butcher, H. R., & van Hoesel, F. H. J. 1992, A&A, 264, 138
Press, W. H., Flannery, B. P., Teukolsky, S. A., & Vetterling, W. T. 1986, Numerical Recipes (Cambridge: Cambridge Univ. Press)
Rogers, F. J., & Iglesias, C. A. 1992, ApJ, 401, 361
Stauffer, J. R. 1991, in Angular Momentum Evolution of Young Stars, ed. S. Catalano & J. R. Stauffer (Dordrecht: Kluwer), 117
Tassoul, M. 1980, ApJS, 43, 469
Toutain, T., & Fröhlich, C. 1992, A&A, 257, 287
Ulrich, R. K. 1986, ApJ, 306, L37
Vandakurov, Yu. V. 1967, AZh, 44, 786; English translation, Soviet Astron.—AJ, 11, 630